IDENTIFICATION OF THE LONGITUDINAL STABILITY AND CONTROL PARAMETERS OF THE YT-2B AIRPLANE

B. J. Eulrich, et al

Calspan Corporation

Prepared for:

Naval Air Development Center

November 1974

Calspan

IDENTIFICATION OF THE LONGITUDINAL STABILITY AND CONTROL PARAMETERS OF THE YT-2B AIRPLANE

B.J. Eulrich and C.L. Mesiah

Calspan Report No. AK-5215-F-1

Prepared For:

NAVAL AIR DEVELOPMENT CENTER
WARMINSTER, PENNSYLVANIA 18974

NOVEMBER 1974
CONTRACT NO. N62269-72-C-0702
FINAL REPORT

**Approved for public release;
distribution unlimited.**

Calspan Corporation

FOREWORD

This report was prepared by Calspan Corporation (formerly Cornell Aeronautical Laboratory, Inc.), Buffalo, New York, for the Naval Air Development Center, Warminster, Pennsylvania. The work was performed under Contract No. N62269-72-C-0702, Project No. 2429/72, "T-2 Stability and Control Investigation." Technical monitoring was initially performed by Mr. Arthur Schuetz and later by Mr. A. Piranian (NADC). Mr. C. Mesiah was the Project Engineer for Calspan and Mr. B. J. Eulrich the Principal Investigator.

The authors wish to express their appreciation to Mr. E. G. Rynaski and Dr. R. T. N. Chen for their many valuable suggestions and discussions during the course of this work and to Mrs. J. Martino for her assistance in the preparation of this report.

TABLE OF CONTENTS

LIST OF ILLUSTRATIONS

LIST OF ILLUSTRATIONS (cont.)

LIST OF TABLES

Section I

INTRODUCTION

This report presents the results of a program undertaken with the Naval Air Development Center (NADC) to analyze flight test data obtained from a Navy YT-2B aircraft, instrumented and operated by NADC. The objectives of this program are to estimate the longitudinal stability and control parameters of the YT-2B, from digitally recorded flight data, collected and supplied by NADC, using an iterated Kalman filter/fixed-point smoother parameter identification algorithm. A linear, constant coefficient, small perturbation equations-of-motion model is used to represent the characteristics of the YT-2B.

The data consists of a total of seventeen flight records: five records at a low speed landing approach configuration and twelve at a higher speed configuration with Mach number around .6. From this group, three low speed and five high speed records were initially selected as the most promising for further data analysis. The results reported herein are primarily those obtained using the low speed flight records. These results correlated favorably with each other and with the initial parameter estimates supplied by NADC. Inaccuracies in the estimated parameters and differences between parameters extracted from different flight records are discussed and straightforward solutions posed.

The organization of this report is as follows: A brief description of the identification algorithm and the mathematical model of the YT-2B is first presented, followed by some general comments related to the flight data. The identification results and conclusions and recommendations follow. Tables and figures are presented at the end of the report for the reader's convenience.

Section II

IDENTIFICATION ALGORITHM

The general problem of estimating stability and control parameters from flight test records can be viewed as one of fixed-point smoothing, that is, estimating both the unknown parameters and the initial condition of the aircraft from the data. With this as a starting point, the estimation philosophy may then be divided into two major groups: Bayesian and non-Bayesian. The difference between these groups is that Bayesian philosophy can take into account a priori information about the data of unknowns, whereas non-Bayesian does not. The Bayesian philosophy assumes that the entire information available to an estimator is contained in the a posteriori density function; that is, the density function of the unknowns given the data.

With the Bayesian philosophy, two estimation criteria can be considered:

(1) The minimum variance or minimum mean squared error criterion; the resulting estimator is the conditional mean, that is, the expected value of the a posteriori density function, or

(2) Maximum likelihood (Bayesian) or most probable estimate, which is the mode of the a posteriori density function.

The identification algorithm used here was developed in Reference 1 using the mean squared error criterion with appropriate Gaussian assumptions. By annexing a constant parameter vector model of unknowns to the aircraft state equations, the recursive algorithm which results is a nonlinear iterated Kalman filter/fixed-point smoother. The nonlinear filter is a form of an extended Kalman filter utilizing a "local iteration" scheme between successive measurements to reduce errors in linearizing the equations of motion and measurement system models by improving the reference trajectory. This improvement is accomplished by smoothing each measurement data point backwards in time one point and re-linearizing. In addition, the outputs of the filter at

each data point can be used in a fixed-point smoothing algorithm to produce a better smoothed estimate of the unknown parameters and initial condition of the aircraft. The algorithm is summarized in Appendix A.

This technique is both a response error and an equation error minimization technique under the usual Gaussian assumptions in the error sources. That is, the technique adjusts the parameters of the model so as to minimize the "weighted" errors between both the measured responses (accelerations included) and the error in formulating the equations of motion of the airplane. The weighting in the measurements is selected to be compatible with the accuracy of the instrumentation and recording system, whereas the weighting of the equation error is compatible with the error in the mathematical model of the airplane. These error sources are commonly referred to as the measurement and process noise, respectively. Although these sources of error are modeled as white, Gaussian and independent in the identification algorithm with covariances R and Q, respectively, they can also be considered as artificial approximations to non-random type errors such as nonlinearities in the model or lags in the instrumentation system, for example, and as such serve as effective weighting matrices.

The selection of these noise statistics in particular is an iterative process which is carried out in practice by observing the residual sequences (measurement data minus predicted measurements) of the filtering operation and adjusting the statistics as required to obtain consistency between the predicted and actual dispersion of the residuals. If the model is correct (implies both form and statistics used), the actual dispersion of the residuals should be zero mean, white and consistent with their theoretically calculated statistics. Two indicators are available:

(1) Visual inspection of the residuals in the form of time history plots; and

(2) Estimation of R and Q from the residuals using covariance matching techniques ($\hat{R}$ and $\hat{Q}$).

R and Q are estimated by the covariance matching technique by approximating the actual residual covariance by its "sample covariance" and by using the relationships between this residual covariance and the R and Q matrices in the identification algorithm. If the model is correct and the records sufficiently long, these estimates serve as a form of hypothesis test to determine if the initial R and Q were selected properly or if not, a guide to further "tuning."

Two other pieces of information are required to perform the identification. These are:

- Initial estimates of parameters and states
- Variance of the initial estimate (P_0).

The selection of these items are discussed in the results section.

Section III

MATHEMATICAL MODEL AND FLIGHT RECORDS ANALYZED

Model of YT-2B

The rigid body, three-degree-of-freedom linearized longitudinal equations of motion model used to describe the recorded small perturbation motions of the YT-2B for identification purposes is given in Table 1. Also included are the measurement system model and appropriate definitions. This model is essentially equivalent to the one supplied by NADC (which is the standard "BuAer type" stability axes systems model) except that the units are different and the unknown stability and control parameters to be identified are completely aerodynamic in origin. In particular, the units for angular measurements are degrees, linear velocities and linear accelerations have the units of feet and the X_α, Z_α and Z_V stability parameters do not include kinematic terms. The moment parameters are primed, for example M'_q, indicating that the effects of $C_{m_{\dot\alpha}}$ have been lumped into these parameters. Y_o, M'_o and Z_o are used to compensate for out of trim or improperly chosen reference conditions.

As shown in Table 1, eight measurements are modeled. These consist of perturbation variables in pitch attitude ($\Delta\theta_m$), true airspeed (ΔV_m), pitch rate (q_m), angle of attack ($\Delta\alpha_m$), z -stability axis linear acceleration (Δa_{z_m}), two angular acceleration measurements ($\dot q_{1_m}$, $\dot q_{2_m}$) and x -stability axis linear acceleration (Δa_{x_m}). Bias parameters, which are subscripted with a small b, are also included in each measurement.

The perturbation measurements supplied by NADC were formed by subtracting an appropriate reference condition from each total flight measurement and using the following transformation to obtain the perturbation stability axis linear acceleration measurements:

$$\begin{bmatrix} \Delta a_x \\ \Delta a_z \end{bmatrix} = \begin{bmatrix} \cos\alpha_t & \sin\alpha_t \\ -\sin\alpha_t & \cos\alpha_t \end{bmatrix} \begin{bmatrix} n_x \\ n_z \end{bmatrix} - \begin{bmatrix} a_x(t_o) \\ a_z(t_o) \end{bmatrix} \qquad (1)$$

where n_x, n_y are the body reference axes accelerometer measurements, a_t is trim angle of attack and $a_x(t_o)$, $a_z(t_o)$ are used to develop perturbation variables.

Flight Records Analyzed

Seventeen flight records were supplied by NADC. For reference purposes, these consisted of five low speed records in the landing approach configuration, numbered 2 through 6, and twelve at a higher speed configuration, labeled 7 through 19 (except 15). Of these, three low speed records (2, 5, and 6) and five high speed records (10, 12, 13, 18, and 19) were initially selected as the most promising for identification purposes. The flight conditions for each record are summarized in Table 2. All records were at a sample rate of 20 samples per second.

The initial values for the coefficients of the equations of motion were supplied at V_t = 236 fps and V_t = 679 fps. These initial values were converted to the parameters of the model given in Table 1 and also updated to be closer to the actual flight condition for comparison purposes. These values, which served as initial estimates, are given in Table 3. In all cases, γ_t was assumed equal to zero.

Section IV

GENERAL COMMENTS

Prior to discussing the results in the next section, a few general comments about the flight data and a discussion of problem areas which were uncovered in analyzing the low speed records are in order. This will provide a proper perspective for interpreting the identification results. Specifically, four potential problem areas are worthy of discussion since these are considered partly responsible for inaccuracies in the estimated parameters and the differences between parameters extracted from different flight records.

The first is the uncertainty of the actual elevator control input applied to the airplane. It is well known that the control input time history recorded for these flight records is extremely noisy and is not the control input applied. This is readily apparent when observing that the flight variables, such as q , α and $\dot{q}$, for example, in most of the records have for all practical purposes reached a steady state but the measured control input has not. The difficulty is not so much the high frequency content of the control input noise but low frequency components which are within the bandwidth of the airplane and have a signal strength which is sufficiently large compared to the actual control input. These low frequency components can be observed by comparing the flight responses generated using the identified parameters in the model with the flight data, by filtering the control input to reduce the high frequency noise components or by observing the residuals in the identification technique. If δ_e is not filtered, the high frequency components do of course affect the measurement noise levels which should be used on the acceleration measurements, particularly Δa_z and $\dot{q}$. This error, of course, is a modeling error which should properly be construed as a source of process noise.

For example, the measured control input, δ_{e_m} , can be modeled as the true control, δ_e , plus additional noise, w , as shown in Equation (2) below. Solving Equation (2) for δ_e

$$\delta_{e_m} = \delta_e - w \tag{2}$$

and substituting the results in the pitching moment equation yields

$$\dot{q} = M'_\alpha \alpha + M'_q q + M'_{\delta_e} \delta_{e_m} + \underbrace{M'_{\delta_e} w}_{\text{process noise}} \tag{3}$$

where the $M'_{\delta_e} w$ term represents the equation error or process noise due to the error in measuring the control input. The next problem is to determine if the noise term is white or colored and its variance. If it is colored, then a shaping filter driven by white noise can be used to model the error term where the parameters of the filters are themselves unknown constants to be identified or else they could be modeled as random. Assuming that the noise is stationary and its characteristics do not change with the application of a control input, the characteristics of the noise term can be obtained from the sample power spectral density (PSD) of the δ_{e_m} with and without the control input applied if the record is sufficiently long to provide meaningful results. For example, this was done for records 6 and 13, but the complete time history was used for records 2, 5 and 18. The results are given in Figures 1a through 1g. These PSD plots serve as a guide in the selection of the process noise level to account for the noise in the control input measurement.

It should be realized that w is acting like an unknown forcing input to the airplane model, similar to an unknown gust input. Consequently, in generating time history responses to compare with the flight data, an estimate of the unknown forcing function time history, $\hat{w}(t)$, should be included in the model, especially if $w(t)$ has very low frequency components. An estimate of $w(t)$ is directly available in the identification technique if a shaping filter is used in the model, as described above. If not, $\hat{w}(t)$ can be generated using the algorithm developed in Reference 1.

Of course, the objectives here are to identify the stability and control parameters of the YT-28, not the characteristics of the noise corrupting the control input time history unless it becomes necessary to do so. Less sophisticated approaches include the following:

(1) Do nothing. Use the δ_e as measured and adjust the measurement noise statistics accordingly.

(2) Similar to (1), except in addition use a constant level of white process noise as indicated by the PSD plots of the control input.

(3) Similar to (1), except first filter δ_e to eliminate the high frequency components of noise.

(4) Similar to (3) above, but in addition use a constant level of white process noise to compensate for the low frequency content of the noise. The level is initially established from the PSD plot of the control input measurements as described above.

(5) Conjecture about what the actual control input was and modify accordingly.

Because of the limited scope of this investigation and other possible instrumentation difficulties discussed below, approaches 3 and 5 were taken initially, followed by approach 2. In particular, the control input on the low speed records was filtered with a "nonrealizable" digital filter which has the frequency characteristics of two cascade fourth-order Butterworth filters, but with no phase shift, with a cutoff frequency of 3.5 Hz. For record 6, it was also conjectured that the control was actually equal to a constant, before and after the application of the pulse type input, and was therefore set equal to the sample mean of the input. The actual and filtered inputs are shown in Figure 2 for comparison. Also shown are the inputs filtered with a cutoff frequency of 2 Hz. A common cutoff frequency of 3.5 Hz was selected by observing the PSD plots of the control inputs so as not to destroy the signal content and also to preserve the sharp edges of the pulse type input of record 6. Clearly, a lower frequency could be used for records 2 and 5. In actuality, little differences were noted in the "major" parameters identified for the low speed records with the use of the filtered or unfiltered control input, if the measurement noise statistics were adjusted to compensate (improperly) for this added error.

For the high speed records, this problem is more serious because of the smaller control input amplitudes with the same level of noise and the increased bandwidth of the airplane.

The second problem is concerned with an inconsistency between the normal stability axis linear acceleration measurement (Δa_z) and the angle of attack vane measurement (α_V). This inconsistency is very apparent when examining the residuals in the identification technique or by comparing generated responses with the flight data. It has the features of a phase shift between the two measurements or a possible phase lag and scale factor error in the vane measurement. The error is definitely nonrandom and the resulting parameter estimates, specifically M'_α, M'_{δ_e}, M'_q, Z_{δ_e} and X_α, are dependent upon the noise levels assigned to these measurements. This presents difficulties in establishing the proper weighting for these measurements (measurement noise) because they must now compensate for the non-random nature of these errors. However, one would suspect the error to be in the α_V measurement and indications are given below to support this suspicion, although conclusive evidence is lacking.

A third problem is associated with the use of stability axes perturbation variables, especially the Δa_x stability x-axis linear acceleration measurement. It turns out that the derivation of an accurate Δa_x measurement from the n_x and n_z body reference axes linear accelerometers requires an accurate knowledge of trim angle of attack (α_t). The transformation is given by Equation (1). Usually, during the short period portion of the flight record, $|\Delta n_z| >> |\Delta n_x|$, and from Equation (1) it is seen that an error in α_t can cause large errors in Δa_x during this portion of the record.

This problem was detected in an attempt to match the Δa_x measurement through the short period portion of the records. Fair matches were obtained with the inclusion of an X_{δ_e} parameter, but the value extracted was unrealistically large. For example, the results given in the following

table were obtained. The value of X_{δ_e} identified was around the same order

Para.	Record 2		Records 5 and 6		
	Initial	Estimated	Initial	5 Estimated	6 Estimated
X_α	-.205	-.386	-.172	-.25	-.27
X_{δ_e}	0	.325	0	.14	.55

of magnitude as X_α , which is absurd! It is now clear that the δ_e time history looked sufficiently close to the error introduced by the transformation (that is, the $\sin\alpha_t\ n_z$ term) to partially compensate for its effect. Excluding the X_{δ_e} parameter and using the Δa_x measurement, could, of course, introduce errors in the X-force parameters extracted, depending upon the level of measurement noise statistics. Adjusting the measurement noise assigned to Δa_x to compensate for this error can be done, but if a large value is required with respect to the other measurement noise statistics, not using the measurement at all provides the same effect. Therefore, the latter has been chosen. Unfortunately, this reduces the ability to extract the X_V and X_α stability derivatives accurately.

A possible error in α_t is also supported by two additional pieces of information. At the beginning of each flight record, where the airplane was known to be near trim and level flight with $\gamma \cong 0$, the pitch attitude and absolute angle of attack were differing by as much as 3.5 degrees. Since

$$\gamma = \theta - \alpha \text{ for } \phi = 0,$$

an offset in θ , α or both, is indicated. Additionally, from information supplied by NADC (Reference 2) concerning the instrumentation calibration it was noted that the inclination of the YT-2B nose boom was calibrated with respect to a "mean wing chord line" and not the fuselage reference line. Although the angular difference is small, this could be a source of error if the linear accelerometer package is aligned to the fuselage reference line.

The difficulties in resolving the aforementioned problem are for the most part due to the use of "perturbation" flight variables, which were supplied and hence used in the equations of motion model and measurement system model. From Table 1, it is seen that in actuality there is no mechanism to identify a true offset in the α_v measurement so as to determine α_t more accurately. The use of a different model is therefore recommended for future flight test data analysis at these flight conditions. One such model which would suffice employs total flight variables, has linear dimensional aerodynamics (including thrust) but nonlinear kinematics and incorporates a nonlinear time varying stability to body axis transformation in the measurement system to model the body reference axis accelerometer measurements (n_x and n_z) directly. With additional biases modeled in the measurement system to be identified as unknowns, this model will provide a mechanism by which to identify an offset in α_v so as to rectify the above problem. For example, this model is briefly outlined in Equations (4) and (5) below.

Equations of Motion:

$$\begin{aligned} \dot{V} &= X_a - g \sin\gamma \\ \dot{\alpha} &= Z_a + \frac{g}{V}\cos\gamma + q \\ \dot{q} &= M_a \\ \dot{\theta} &= q \end{aligned} \tag{4}$$

Acceleration Measurements:

$$\begin{aligned} n_x &= X_a \cos\alpha - Z_a V \sin\alpha \approx X_a - Z_a V\alpha \\ n_z &= X_a \sin\alpha + Z_a V \approx X_a\alpha + Z_a V \end{aligned} \tag{5}$$

where

$$X_a \triangleq X_o + X_V \Delta V + X_\alpha \Delta\alpha + etc.$$

$$Z_a \triangleq Z_o + Z_V \Delta V + Z_\alpha \Delta\alpha + etc.$$

$$M_a \triangleq M_o + M_V \Delta V + M_\alpha \Delta\alpha + etc.$$

$$\Delta V = V - V_o \text{ , } etc.$$

$$\gamma = \theta - \alpha$$

The last area is an observed phase lag in the angular accelerometer with the application of sharp control inputs like those in record 6. This is in direct agreement with the large phase shift observed and reported in Reference 2 when calibrating this instrument at NADC on the oscillating rate table. The specification for this instrument indicates a natural frequency in the order of 10 Hz, which is low for an acceleration sensor, especially when used to record the motions due to sharp control inputs.

In general, all four problems are more serious for the high speed flight records because of the increased bandwidth of the airplane at this flight condition. The results are discussed next.

Section V

RESULTS

This section presents the identification results obtained using records 2, 5, and 6. Additionally, the results from a rather limited analysis of records 13, 18 and 19 are given. Also cited are the problems discussed in the preceding section. In all cases, unless otherwise indicated, the initial parameter estimates are those given in Table 3. Parameters which have very small effects on the flight responses, and therefore cannot be identified accurately, were held fixed during the identification.

For example, X_q , Z_q and X_{δ_e} were set equal to zero - X_{δ_e} was only identified during assessment of the problems associated with the Δa_x measurement, as discussed previously. Also, it was assumed that the airplane was trimmed at $\gamma_t = 0$, so that X_θ , Z_θ and M'_θ were known exactly. Even if $\gamma_t \neq 0$, the latter two parameters are extremely small and have no apparent effect on the flight responses, especially for the short period type records. Similarly, for a rigid airplane, $\partial C_L / \partial V = 0$, so that Z_V depends only upon the knowledge of V_t . Since its value is somewhat insensitive to small variations in V_t , it also was held fixed at the particular estimated trim condition.

For all cases, biases in pitch rate (q_m) and all the acceleration measurements were identified along with the out-of-trim parameters, X_o , M'_o and Z_o . Since the measurements used are perturbation variables for a selected reference, these biases were extracted differently for each record (as anticipated), and therefore are not presented. The first data points in each record were used as the initial state estimates (tempered with engineering judgment because of the high level of noise) and the variances of these estimates were set equal to the measurement noise variance of the respective state measurements (biases included). The variances of the initial parameter estimator (P_o), which represent the accuracy of these estimates in the form of "a priori" information, were set sufficiently large to insure that the initial estimate had little effect on the final extracted values.

The measurement noise statistics were initially established by means of a "sample variance" calculation on each measurement for all records. The mean value of each measurement, which is required for such a calculation, was "approximated" by using the same digital filter as was applied to the control input. The results, averaged overall records, with anomalies eliminated, are given in Table 4. These values provide an "approximate" estimate to the random component of measurement error and therefore serve as a good initial estimate, more like a lower bound, since they do not account for such things as instrument nonlinearities or dynamics.

It was noted that the noise on the angle-of-attack vane for record 2 was higher than records 5 and 6, which is consistent with the pilot comments indicating the presence of moderate turbulence for this record. Assuming the absence of turbulence in records 5 and 6, the standard deviation of the vertical component of the gust velocity, σ_{w_g} , in the body axes coordinate system, was estimated to be approximately equal to .5 feet per second. This value could serve as a good initial estimate in the selection of the process noise level in using a turbulence model, such as a simplified Dryden model, for example, to account for the effects of the turbulence input during the identification. However, the effects of turbulence at this level on the identification results, if they are neglected, are probably small compared to the other problems cited above and, therefore, a turbulence model was not employed.

Although unknown forcing inputs to the airplane or model of the airplane are known to exist because of the presence of turbulence and the uncertainty of the control input applied, many of the results reported herein assume no process noise (Q = 0). Additionally, the angular acceleration measurement ($\Delta\dot{q}_2$) which was derived from the tail and nose linear accelerometers, was not used in the identification, but the time history matches to this measurement are presented.

Record Number 2 ($Q = 0$):

The identification results for this record are given in Table 5 and typical time history response comparisons with the flight data, using the estimated parameters for the particular cases indicated, are given in Figures 3 and 4. In all cases, the control input was filtered using a cutoff frequency of 3.5 Hz as explained previously. This record has little phugoid excitation (small velocity change) so that parameters such as X_v and M'_v would be hard to identify.

Table 5 presents the identification results of five cases, labeled 2-1 through 2-5, and the measurement noise statistics used to perform the identification. These five results serve to highlight some of the problems discussed in the preceding section. The first case (2-1) uses the Δa_x measurements with X_{δ_e} identified, whereas the other four cases do not, to show the improvement gained in matching the Δa_x response in the former case. Unfortunately, X_α is difficult to identify accurately without the use of this measurement.

For the second case (2-2), the σ -values obtained from the "sample variance" calculation (Table 4), were used for the measurement noise covariance matrix (R), with X_{δ_e} held fixed at zero. The response comparisons with the flight data and the residuals (measurement data minus the predicted estimates) during the identification are shown in Figures 3a and 3b respectively for this case. The unknown forcing input to the model (caused mainly by the uncertainty of the control input), the inconsistency of the $\Delta\alpha$ and Δa_z measurements and the problems associated with Δa_x are readily apparent. The residuals show a definite breakup or deterministic type dispersion, a clear indication of a modeling problem. Figure 4a gives the response comparison with Δa_x for case 2-1 where X_{δ_e} is identified. Comparing this with Figure 3a shows an indication of the problem with Δa_x . Although not shown, the use of the Δa_x measurement without identifying X_{δ_e} provides a similar response match to Δa_x as shown in Figure 3a.

Cases 2-3 and 2-4 show the effects of adjusting the values of the measurement noise statistics, particularly 2-4, where the accuracy of $\Delta\alpha$ is decreased and that of Δa_z increased. Changes in some of the major parameters are evident. Figure 4b gives the response comparisons with $\Delta\alpha$ and Δa_z for case 2-4; the other responses were similar to case 2-2. Comparison of Figure 4b with the $\Delta\alpha$ and Δa_z response matches in Figure 3a provides another indication of the $\Delta\alpha$ and Δa_z inconsistency. Pickup of large wind components by the angle-of-attack vane was not considered in this comparison because the results were similar for record 5, which was obtained in only slight turbulence on a different day.

For the last case (2-5), the measurement noise statistics were selected to be equal to the diagonal elements from the estimator for the measurement noise statistics ($\hat{R}$) to make the two consistent. This is not exactly proper, since $\hat{R}$ reflects errors introduced by the unknown input, which is a process noise error, and other non-random type instrument errors and therefore, the estimated values are expected to be different for each record. However, it provides a convenient guide for the selection of R .

The accuracy of the parameter estimates, as given by twice the square root of the diagonal elements of the final covariance ($2\sigma_f$), are presented in the last column of Table 5. Case 2-5 results were used, because the value of the measurement noise statistics is more representative of the errors present in the flight record. Although these values are only approximations because of errors which were modeled improperly, they appear to be very reasonable indications of the estimation accuracy, which is construed as $\pm 2\sigma_f$.

Record Number 5 ($Q = 0$):

Similar to the identification results presented for record 2, a spectrum of five identification cases is presented for record 5. The only difference is that X_V was held fixed at the initial estimate because of the small velocity change in this record. The results are given in Table 6, for the five

cases labeled 5-1 through 5-5, which are in direct correspondence to cases 2-1 through 2-5.

The response comparisons with the flight data and the residuals are given for cases 5-2 (R -sample variance) and 5-5 ($\hat{R}$) in Figures 5 and 7, respectively. For comparison with these time history matches, Figure 6a gives the response comparison with Δa_x for case 5-1, and Figures 6a and 6b gives the response comparisons with $\Delta\alpha$ and Δa_z for cases 5-3 and 5-4, respectively. Conclusions drawn from these results are similar to those briefly discussed for record 2 above.

Record Number 6 ($Q = 0$):

This record, unlike the former two, has a classical pulse type input for excitation of the phugoid. Again five identification cases are presented in Table 7, labeled 6-1 through 6-5 and various response comparisons to the flight data are given in Figures 8 through 11. In all cases, Δa_x was not used.

The first two cases (6-1 and 6-2) used only the first five second short period portion of the flight record and therefore, X_v was held fixed. Also, the control input was filtered with a cutoff frequency of 3.5 Hz. Case 6-1 employed the sample variance computation for R whereas R was adjusted upwards for 6-2. The response comparisons with the flight data are shown in Figure 8 for case 6-2 and indicate the phase lag in $\dot{q}_m$ discussed above, which is the main reason for presenting these cases. Also, the error in the control input is clearly indicated in the q and $\dot{q}$ comparisons.

Cases 6-3 and 6-4 use a modified control input and the first 14 seconds of the flight record. It was conjectured that the elevator surface was actually a constant before and after the application of the pulse, so it was set equal to its average value at these times. There is a danger in doing this because of the presence of an actual input, so that only the first 14 seconds of

this record was used. It appeared as if an input were applied near this time. Case 6-3 employs the sample variance calculation for $\mathcal{R}$, with the exception that $\sigma_{\dot{q}}$ was adjusted upward to account for the phase lag in $\dot{q}$. Case 6-4 uses the diagonal element from the $\hat{\mathcal{R}}$ (measurement noise covariance estimator). There is no guarantee, however, that this was the control input applied. The response comparison with the flight data, which is similar for both cases, and the residuals, are given in Figure 9.

The flight responses for case 6-3 were then compared for the first 28 seconds using a step size (Δt) of 0.1 seconds. Drift was noted in $\Delta\theta$, $\Delta\alpha$ and ΔV . Consequently, X_V and M'_V were identified using the full 28 second portion of the record with the other parameters held fixed at the case 6-3 estimator with Δt = .1. The results are presented as case 6-5 in Table 7 and the response comparisons with the flight data are given in Figure 10. A drift is still noted in the $\Delta\alpha$ response which could be the result of an applied input or a minor parameter which was not estimated, such as Z_θ or Z_q , for example. Figure 11 gives the response comparison with the flight data using the "actual" control input for case 6-5 but at a Δt = .05 seconds for comparison purposes.

Record Number 5($Q \neq 0$)

Record 5 was reanalyzed using approach number 2 described previously. That is, process noise, w, was used to model the uncertainty of the control input as described in Equation (3). The process noise was assumed zero mean, white and Gaussian with a variance level selected from the PSD plot of the control input, Figure 1b. It was assumed that the high frequency portion of the PSD represented noise only, the characteristics of which were similar at the low frequency end. The dashed line in Figure 1b, which is representative of the level selected, gives a process noise standard derivation of

$$\sigma_{\delta_e} = \sqrt{\frac{\Phi_{\delta_e}}{2}} \approx .14 \text{ deg}$$

where the factor of 2 is required because of the definition used between the autocorrelation function and the power spectral density in the PSD computer program

The identification results employing this level of process noise, an unfiltered control input and a level of measurement noise consistent with the R estimates are given in Table 8 as case 5-6. Only the short period and control effectiveness parameters were identified; the others were held fixed at the initial estimates. The results compare favorably with those for Q = 0 and δ_e filtered (Table 6) and the $\pm 2\sigma_f$ values appear to be very reasonable indications of the estimation accuracy.

For Case 5-6, the time histories of the state estimates and the residuals are given in Figure 12. Since an estimate of the unknown forcing function, $\hat{w}(t)$, was not available for incorporation into the model for generating time history responses to compare with the flight data, none is given. However, the state estimates from the iterated Kalman filter and the residuals suffice because they include the effects of process noise. Similar to the results given above, the $\Delta\alpha$ and Δa_z residuals still show an inconsistency. Additionally, the white noise approximation for $w(t)$ may be questionable, although more analysis is required to determine this, partly because of the cause and effect relationships due to the $\Delta\alpha$ and Δa_z uncertainty. If a shaping filter is used to color $w(t)$, the sample rate of 20 per second may be low.

Record Number 5 ($\Delta\alpha$ and Δa_z inconsistency):

As cited above and described previously, an inconsistency appeared to exist between the $\Delta\alpha$ and the Δa_z measurement and this error made it difficult to establish a consistent set of measurement noise statistics. From analysis on record 5, it appeared like a scale factor error in the vane measurement could be responsible. Usually, such an error is the result of wing/fuselage (possibly landing gear) air flow effects and is largest for short booms and low Mach numbers. Unfortunately, the measurement system model in Table 1 did not include a scale factor parameter which could be treated as an unknown to be identified.

However, a model was available from previous identification efforts at Calspan (Reference 3) which uses the kinematic equations of the aircraft and a typical measurement system model in the manner of a strapped-down inertial measuring unit. This model, when used in the identification algorithm, allowed for the estimation of such parameters as biases and scale factors in the instrumentation system, "independent" of the aerodynamic model of the airplane. This is desirable here because of the modeling error caused by the noisy control input. The model is given in Equations (6) and (7) below.

Dynamic Model:

$$\begin{aligned}
\dot{q} &= \dot{q}_m - \dot{q}_b + v_1 \\
\dot{\theta} &= q \\
\dot{u} &= -qw - g\sin\theta + \Delta n_{x_m} - n_{x_b} + v_2 \\
\dot{w} &= qu + g\cos\theta + \Delta n_{z_m} - n_{z_b} + v_3
\end{aligned} \tag{6}$$

Measurement System:

$$\begin{aligned}
q_m &= q + q_b + v_4 \\
\Delta\theta_m &= \theta + \theta_b + v_5 \\
\Delta\alpha_m &= (1 + K_s)\tan^{-1}\left(\frac{w - 23.1q}{u}\right) + \alpha_b + v_6 \\
\Delta V_m &= (u^2 + w^2)^{1/2} + V_b + v_7
\end{aligned} \tag{7}$$

These are the three-degree-of-freedom kinematic equations written in the aircraft body axis coordinate system, where the subscripts m, b, and s imply measurements, biases, and scale factors, respectively. Noise terms are represented by v_1 through v_7.

For application to record 5, biases were used to relate the total flight variables to the perturbation measurements. Additionally, Δn_{x_m} and Δn_{z_m} were approximated by Δa_{x_m} and Δa_{z_m}, respectively, and the noise statistics used are those given in Table 4, with the exception of σ_{a_x}. σ_{a_x} was increased to account for the above approximation. Five biases, $\dot{q}_b$, n_{x_b}, n_{z_b}, q_b and α_b and the scale factor, K_s, were treated as unknowns. The result was a K_s estimated value of .275--surprisingly high!

The time histories of the residuals and state estimates are given in Figure 13. For comparison, the residual for $\Delta\alpha$ obtained by setting $K_S = 0$ is given in Figure 14. It is readily apparent that the scale factor error could be the problem, but the value extracted appears unreasonably high. Of course, the scale factor could be accounting for other unmodeled error sources for this record. However, this does support early suspicions that the inconsistency is indeed in the measurements, but additional analysis would be required to ascertain the exact error source.

It is also interesting to note that the measurement noise statistics for Δq and $\Delta\theta$ in Table 4 are reasonable values. It therefore appears that the larger values obtained from the R estimates for case 5-6 (refer to Table 8), could possibly be due to the assumption of white noise for w being a poor one.

In summary, the results for the low speed records correlate favorably. It is clear, however, that the high level of uncertainty and noise present in these flight records precludes the use of visual prediction to demonstrate the accuracy of the estimated parameters, that is, using the estimated parameters from one record to predict the responses of the airplane to another record. It is believed that the predicted comparisons would be highly subjective and a meaningful criterion by which to interpret the results hard to establish. For example, if the state estimates from the Kalman filter model are used in such a prediction, the high level of process noise required to model the control input uncertainty would clearly "mask out" the effects in the predicted comparisons introduced by the differences in the parameter values between all three flight records.

High Speed Records:

Little effort was devoted to the high speed records. As expected, the problems cited above have been observed to be considerably more serious for these records. Structural vibrations appear higher for these records and the signal to noise ratio present on the control input measurement is much lower

than the low speed records, although the characteristics of the noise appear similar. Also, lags or inconsistencies in the instruments take on added importance because of the higher bandwidth of the airplane.

From the knowledge gained with the low speed records, it was decided to drop analysis on records 10 and 12 because of the extremely low signal level present in the control input for these records and identify only the short period and control effectiveness parameters for the other three records. Referring to Table 2, records 13 and 18 have control inputs which excite principally the short period motion of the aircraft whereas record 19 has persistent pulse type inputs applied.

The identification results are summarized in Table 9. In particular, process noise was used to model the control input noise at a level selected from the PSD plots, Figure 1, for records 13 and 18, and the R-estimator used to establish the level of measurement noise. The Δa_z and $\dot{q}$ measurements were not used for reasons cited previously and because the phase lag in $\dot{q}$ can introduce large errors. For record 19, the control input was filtered at 3.5 Hz, process noise was assumed equal to zero, x_α identified and only the first portion of the record used. Also, R was not adjusted to be consistent with the R-estimator.

The time histories of the residuals and state estimates for records 13 and 18 are shown in Figures 15 and 16, respectively. Response comparisons with the flight data for record 19 are shown in Figure 17. The response comparisons appear good. However, the persistent type control input applied for this record could effectively mask out or hide the free response of the airplane.

These results represent the very first efforts to analyze the high speed flight records and are therefore considered preliminary, at best. Time and money precluded further analysis. However, improvement in the results is very unlikely because of the poor quality of these records.

Section VI

CONCLUSIONS AND RECOMMENDATIONS

Flight test data from a Navy YT-2B aircraft, instrumented and operated by NADC, were analyzed to estimate the longitudinal stability and control parameters of the YT-2B at two flight conditions: a low speed landing approach configuration and a higher speed cruise configuration. The method of system identification employed was a nonlinear iterated Kalman filter/fixed-point smoother identification algorithm. The method also had the capability to adaptively estimate the measurement and process noise level from the flight data. The identification results obtained were good, considering the extremely high level of noise in the flight data.

For the low speed flight records, the parameter estimates correlated favorably with each other and with the initial wind tunnel estimates. The covariance matrix of the parameter estimates also appeared to be a very reasonable indication of the estimation accuracy. Four problems were responsible for the inaccuracies in the estimated parameters and the differences between the parameters extracted from different flight records. They are:

1. Inaccurate knowledge of the actual control input applied.
2. An inconsistency between the angle of attack and normal stability axis linear acceleration measurements.
3. Incorrect Δa_z measurement, caused mainly by an error in the trim angle of attack.
4. Generally very high level of noise in the flight records, due to the flight instrumentation and recording system.

Each of these problems was discussed in the main text of the report and straightforward solutions posed. The inaccurate measurement of the control input is by far the most serious. It was shown that both filtering of the control input and/or modeling the error in the input with process noise, where the level of noise is established from the sample power spectral density of the

control input time history, were very effective and desirable solutions. The latter solution, of course, requires that the identification algorithm be capable of accounting for both response error (measurement noise) and equation error (process noise). It is clear, however, that a properly designed and calibrated instrumentation/recording system would eliminate these unnecessary efforts at the analysis level and improve upon the accuracy of the estimated parameters. Because of the generally poor signal to noise ratio of the control input measurement, meaningful results from the high speed records were not possible.

The following recommendations can be drawn based upon the results of this investigation.

1. Data analysis and flight testing should be done concurrently. Problems detected from the data analysis, such as, modeling or instrumentation deficiencies or improper control input excitation, for example, can be corrected immediately. To do otherwise, can lead to a loss of valuable flight test time.
2. The instrumentation problems cited above should be investigated further; initially however, at the flight instrumentation and recording system level. Specific flights should also be devoted to instrumentation calibration checks. If necessary, the combined airplane/instrumentation system should be modeled.
3. A different longitudinal model of the airplane should be used for further data analysis at these flight conditions. The model used in this investigation is deficient because of the inherent inaccuracy in the small perturbation body to stability axis transformation, especially if trim angle of attack is not known.
4. Further analysis should be done to obtain estimates for the longitudinal parameters at the cruise configuration and the lateral-directional characteristics at low angles of attack, but only after the instrumentation problems have been corrected.

REFERENCES

1. R.T.N. Chen, B.J. Eulrich and J.V. Lebacqz, "Development of Advanced Techniques for the Identification of V/STOL Aircraft Stability and Control Parameters," Calspan Report No. BM-2820-F-1, August 1971.

2. Memorandum to Supt., Aerodynamics and Propulsion Division, Via C. J. Mazza, from A. J. Schuetz, Subject: IR Task R000-01-01/ MF-9-01, Aircraft Dynamics Identification Program, Calibration of YT-2B instrumentation for . . ." Naval Air Development Center Memo No. 3015:AJS, 7 November 1972.

3. B. J. Eulrich and N. C. Weingarten, "Identification and Correlation of the F-4E Stall/Post-Stall Aerodynamic Stability and Control Characteristics from Existing Test Data," Calspan Report No. AK-5126-F-1, November 1973.

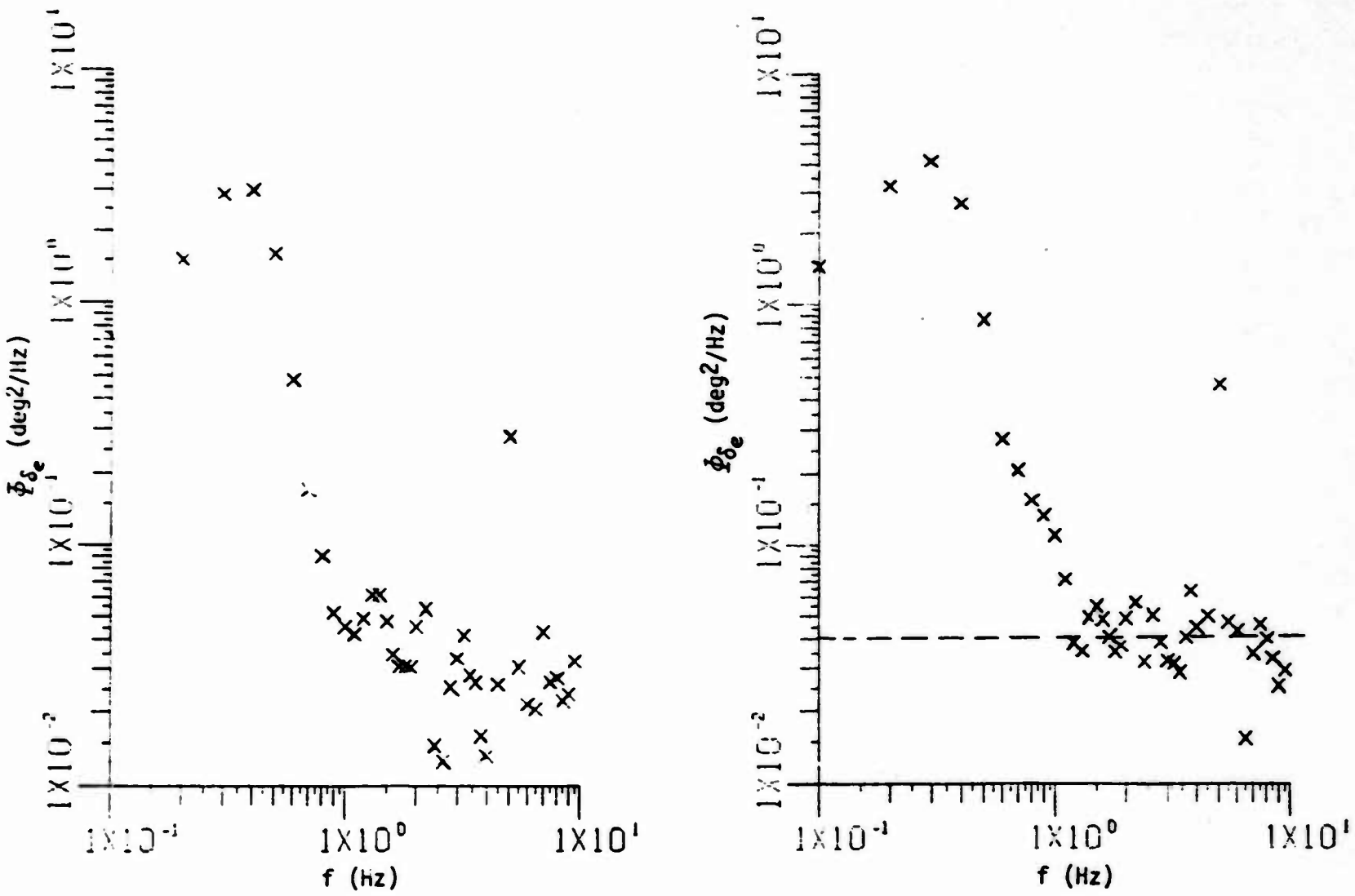

a. Record No. 2

b. Record No. 5

Figure 1 CONTROL INPUT POWER SPECTRAL DENSITIES FOR SELECTED FLIGHT RECORDS

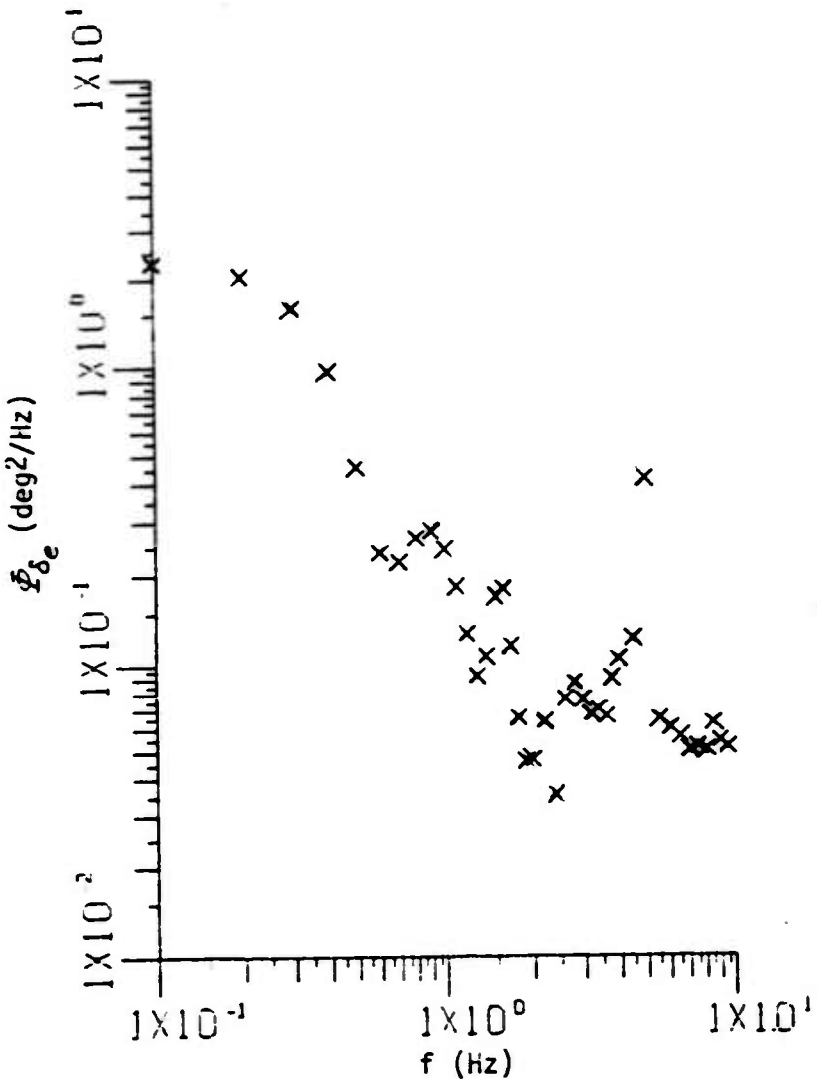

c. Record No. 6

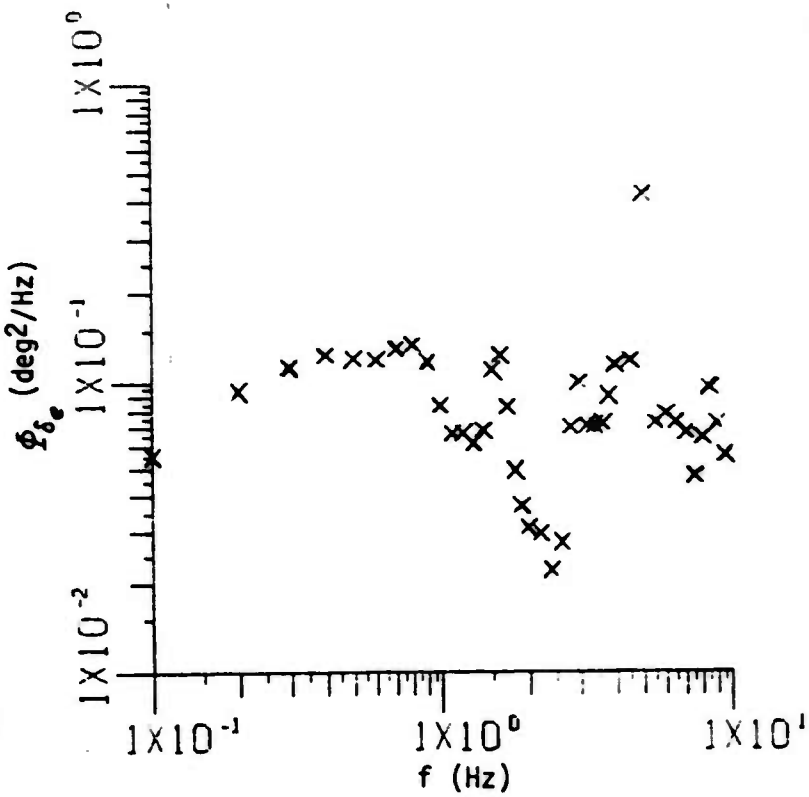

d. Record No. 6 - Excluding Portion of Record with Pulse Input

Figure 1 (cont'd) CONTROL INPUT POWER SPECTRAL DENSITIES FOR SELECTED FLIGHT RECORDS

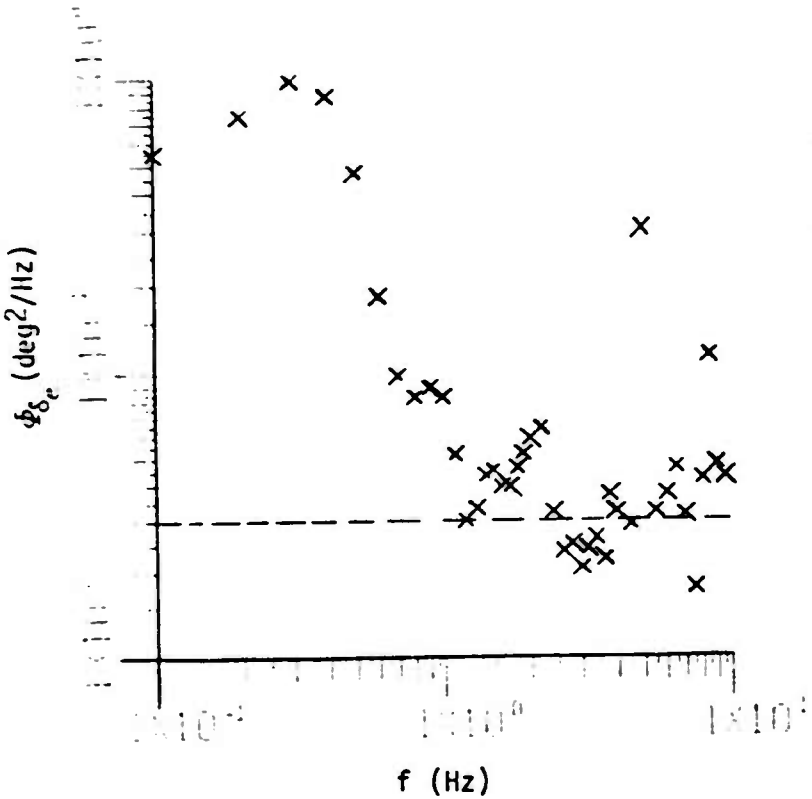

e. Record No. 13

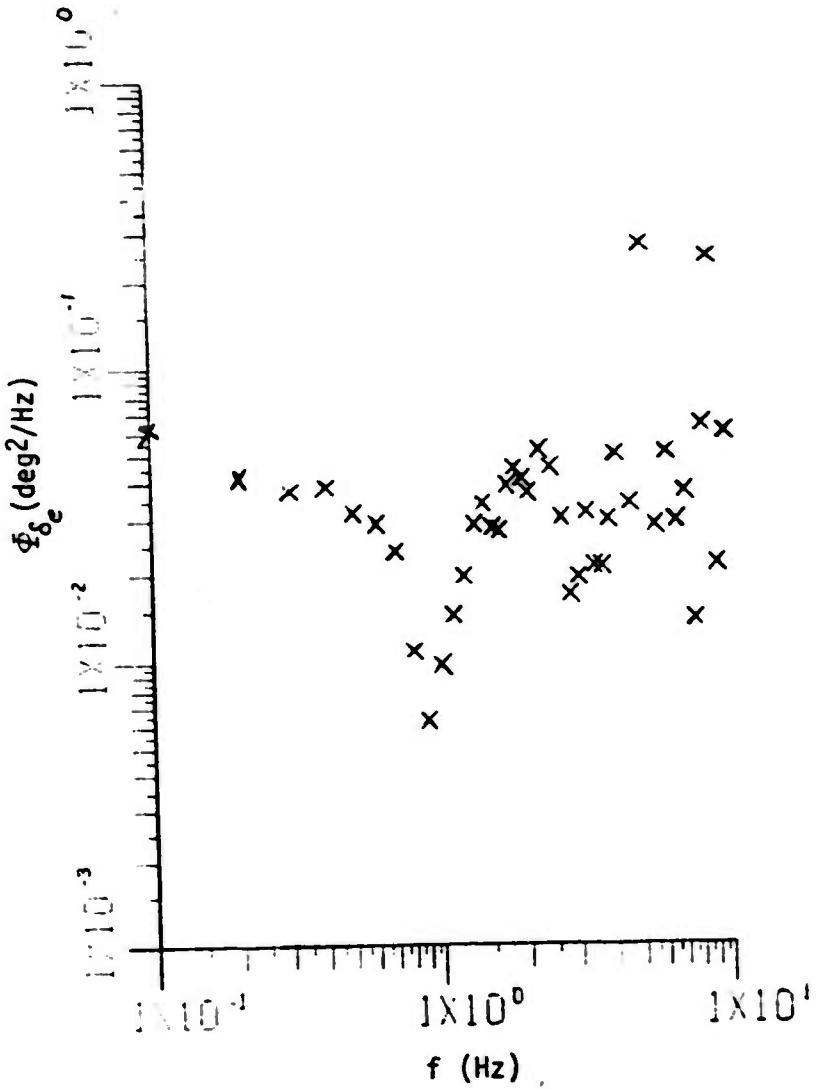

f. Record No. 13 - Excluding Portion of Record where Control Applied

Figure 1 (cont'd) CONTROL INPUT POWER SPECTRAL DENSITIES FOR SELECTED RECORDS

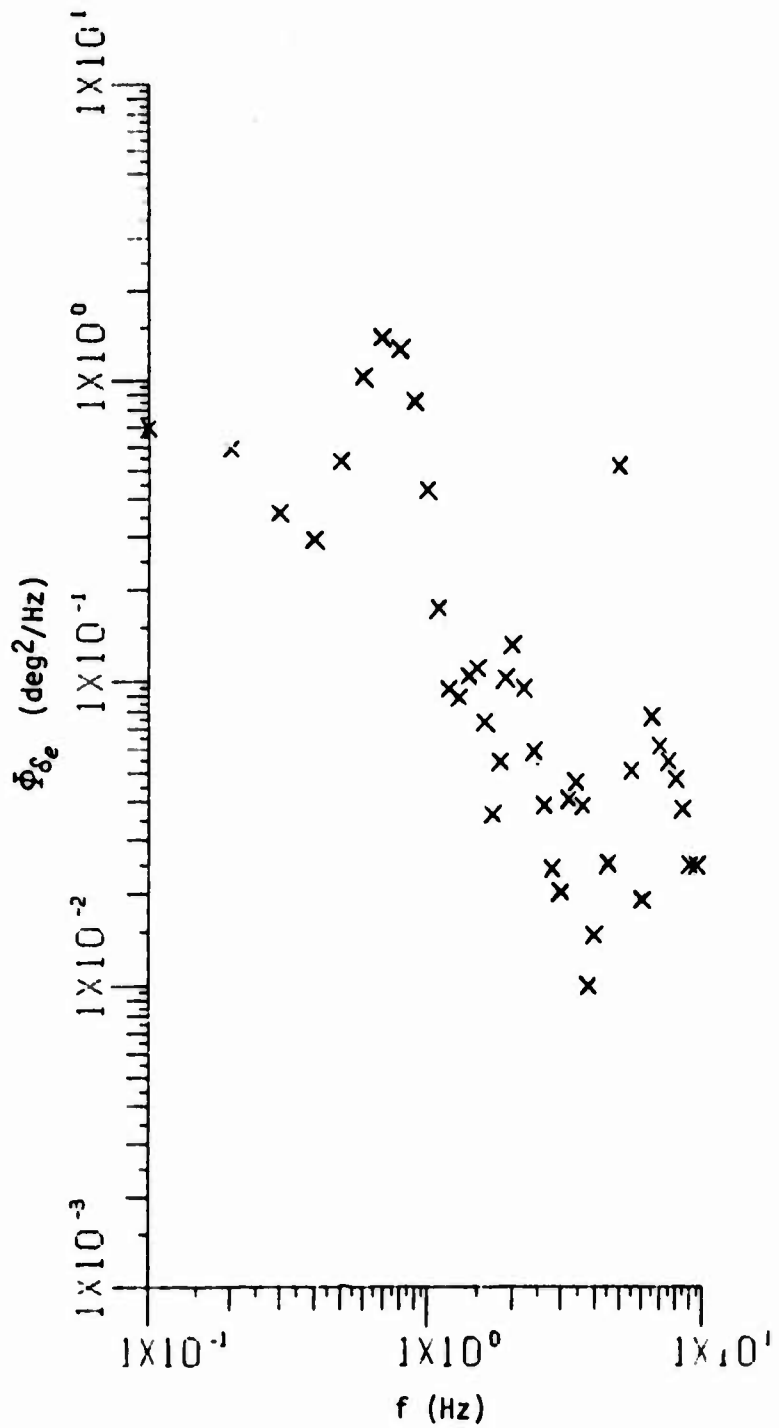

g. Record No. 18

Figure 1 (concl'd) CONTROL INPUT POWER SPECTRAL DENSITIES FOR SELECTED FLIGHT RECORDS

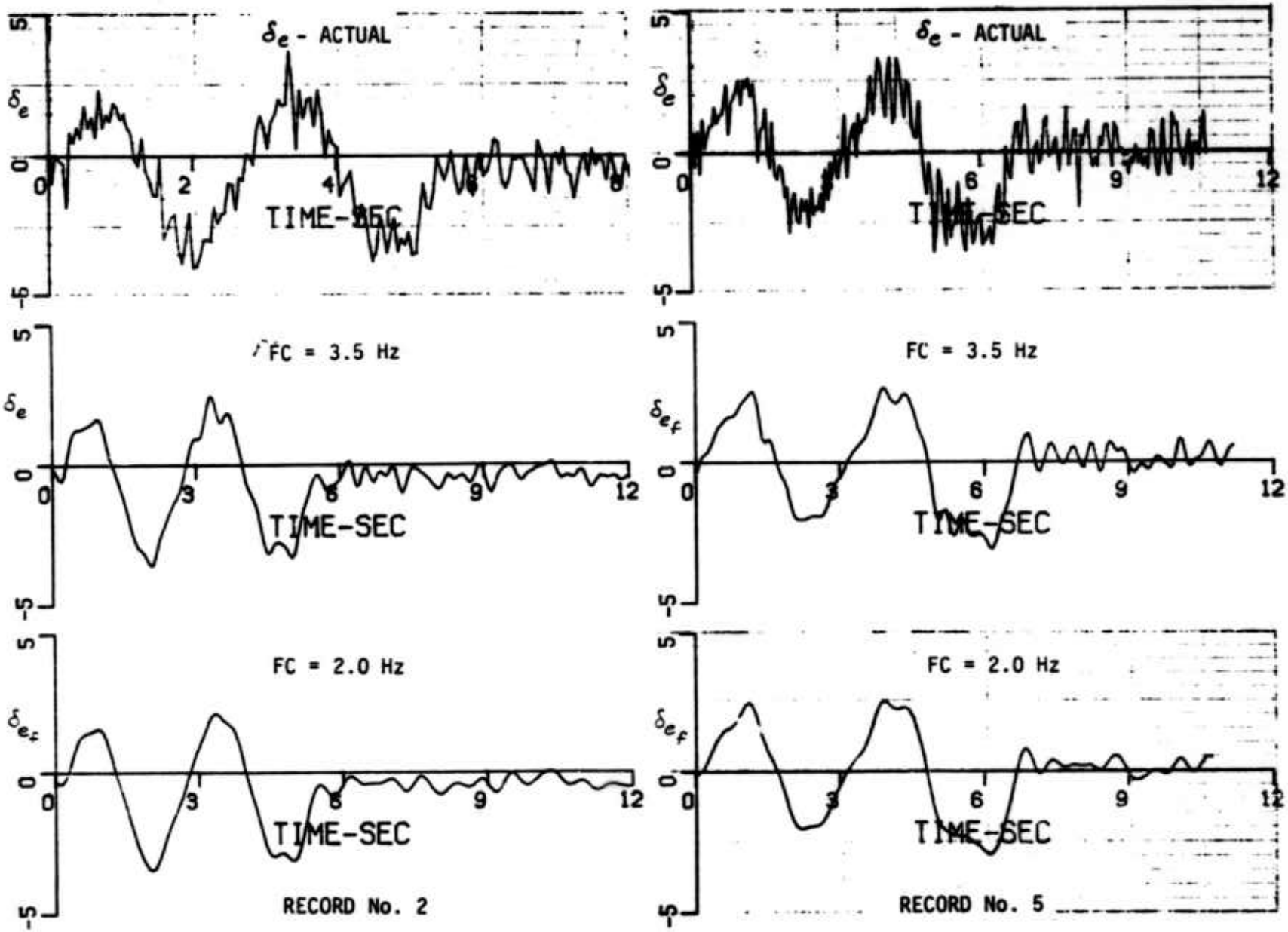

Figure 2 ACTUAL AND FILTERED CONTROL INPUTS FOR RECORDS 2,5 AND 6

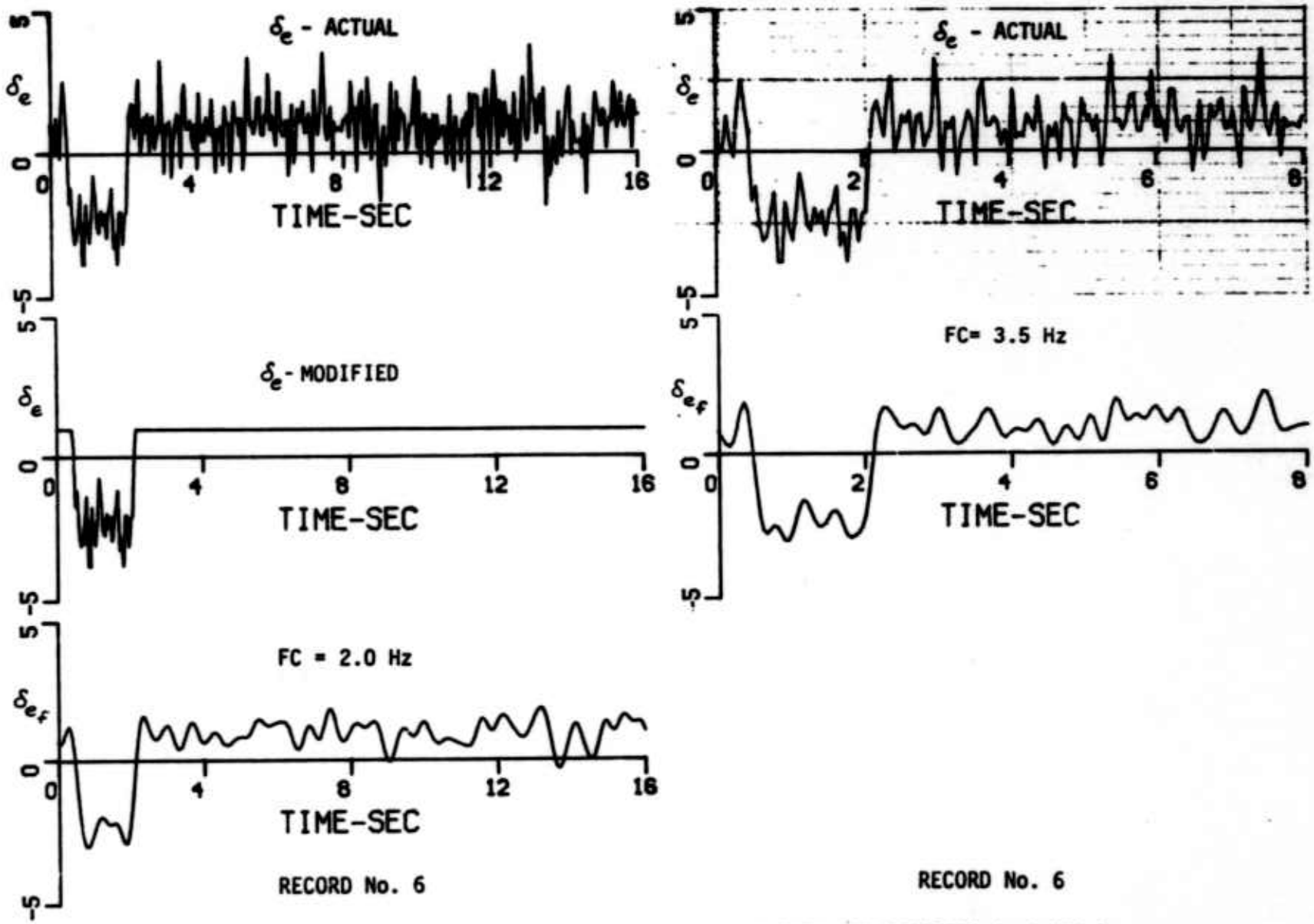

Figure 2 (cont'd) ACTUAL AND FILTERED CONTROL INPUTS FOR RECORDS 2, 5 AND 6

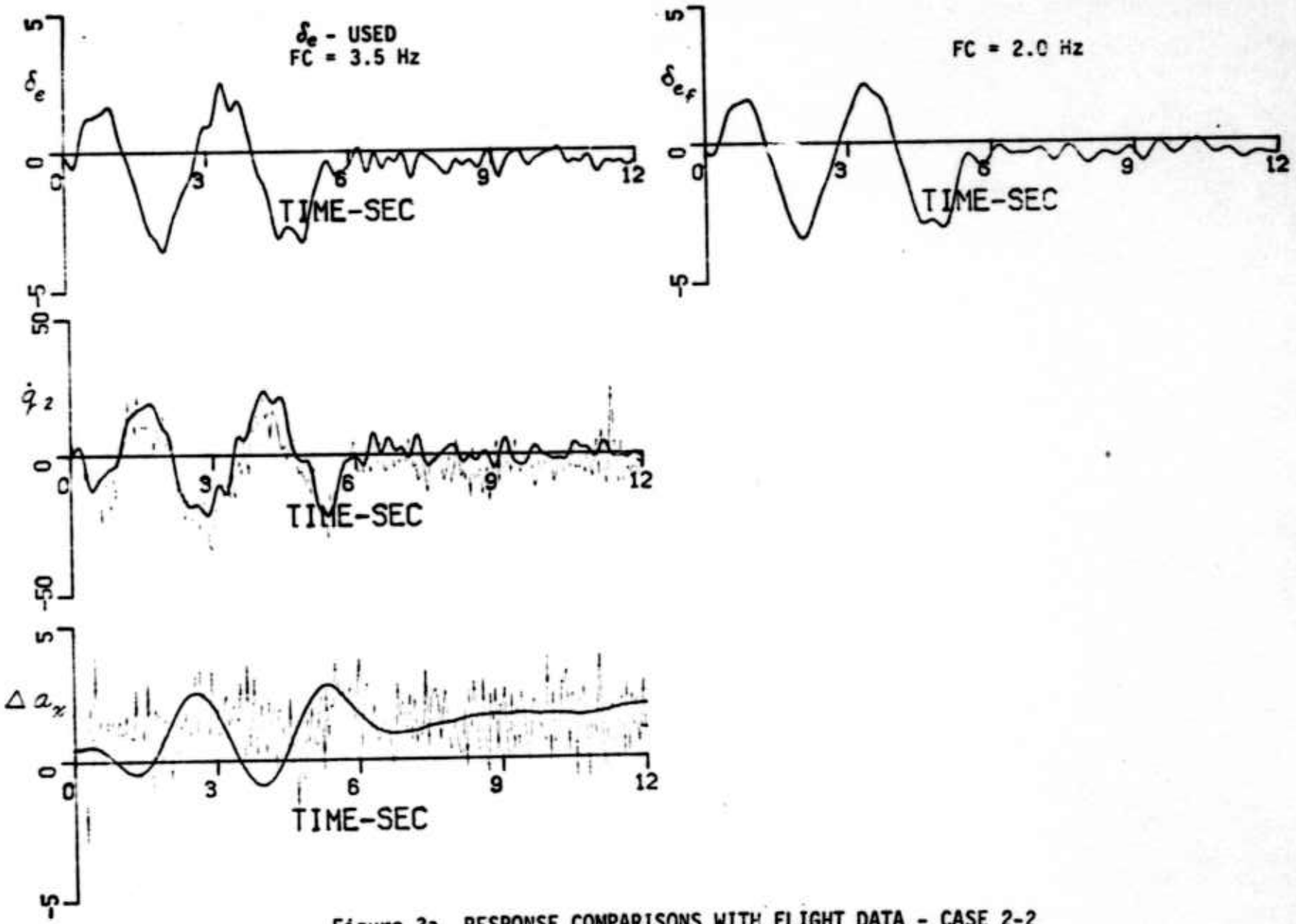

Figure 3a RESPONSE COMPARISONS WITH FLIGHT DATA - CASE 2-2

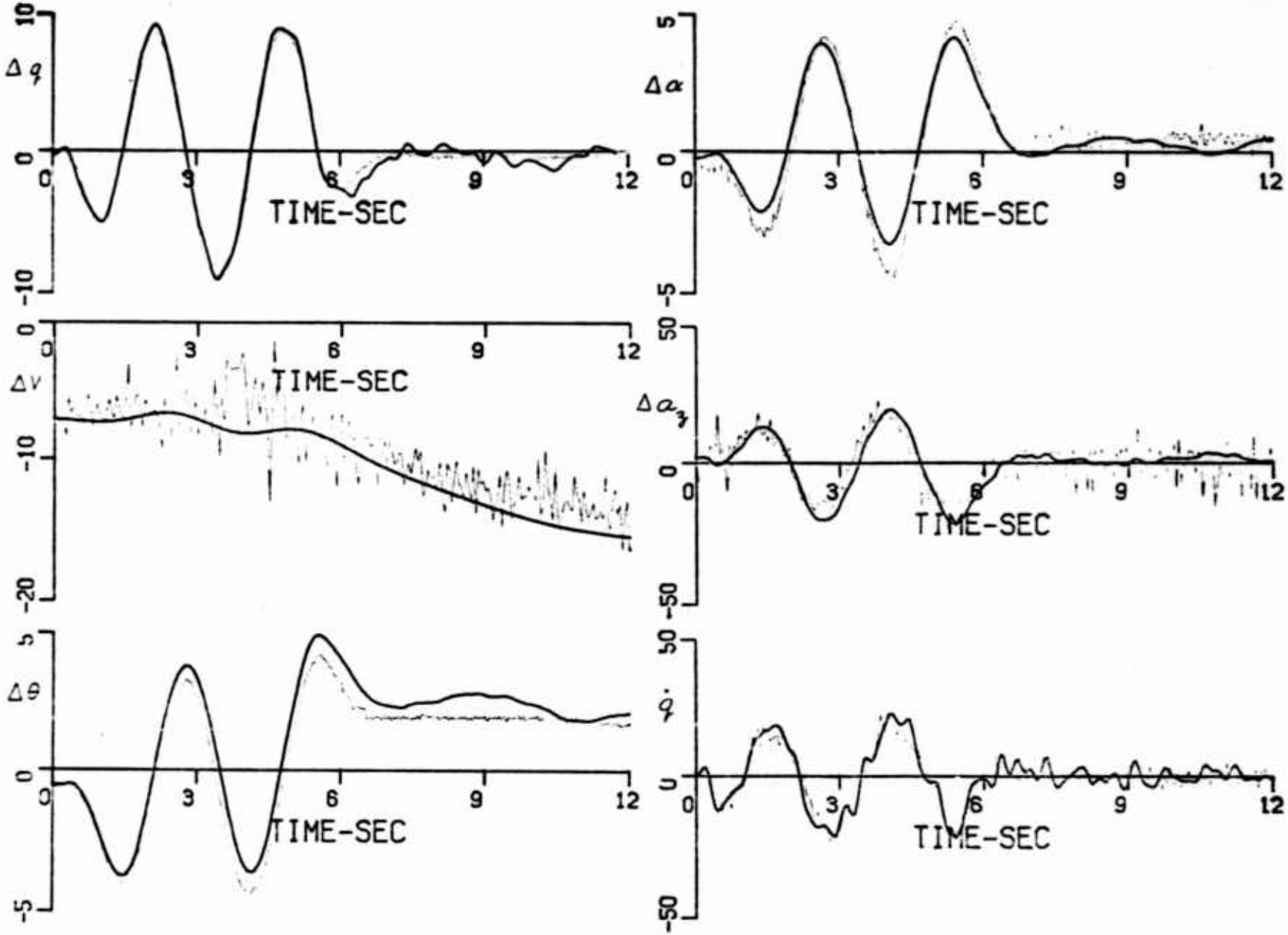

Figure 3a (cont'd) RESPONSE COMPARISONS WITH FLIGHT DATA - CASE 2-2

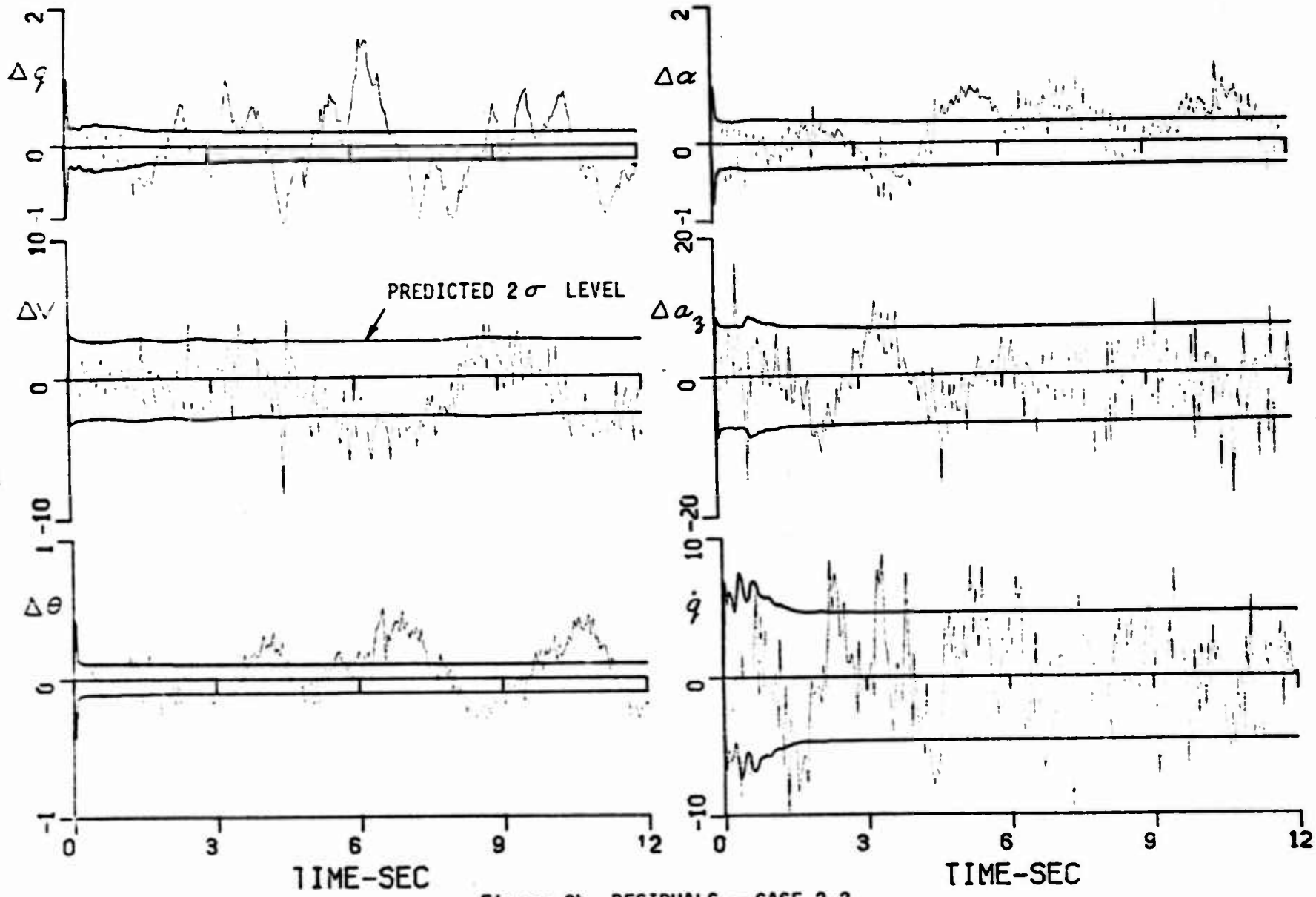

Figure 3b RESIDUALS - CASE 2-2

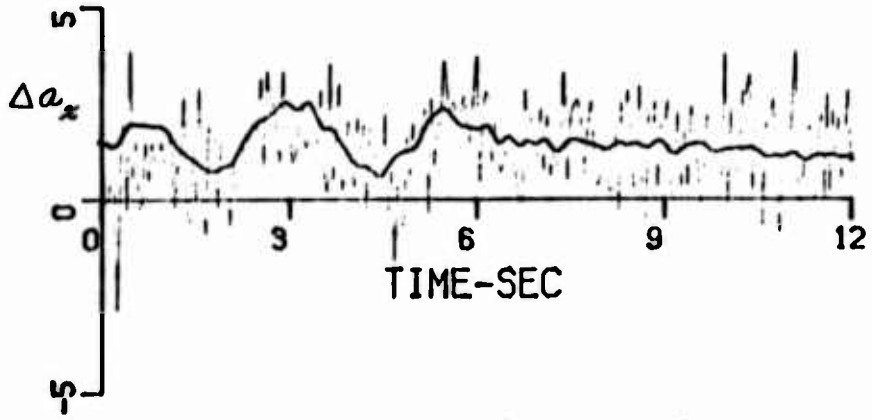

a. Response Comparison with Δa_x - Case 2-1

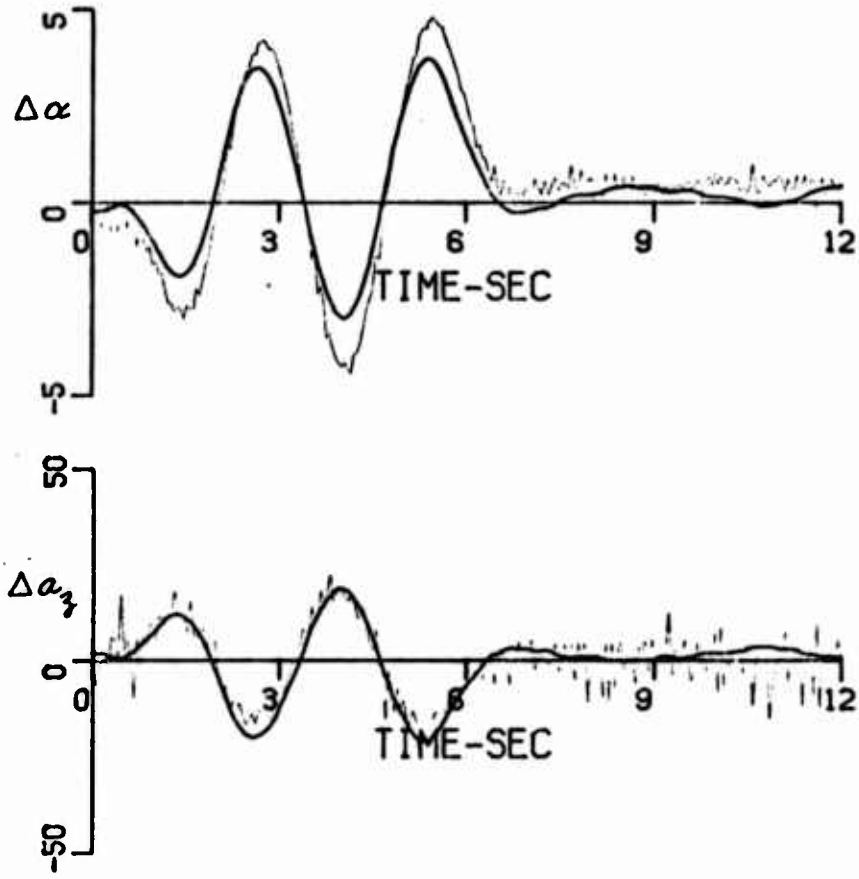

b. Response Comparisons with $\Delta\alpha$ and Δa_z - Case 2-4

Figure 4 RESPONSE COMPARISONS WITH PERTINENT MEASUREMENTS FOR CASES 2-1 AND 2-4

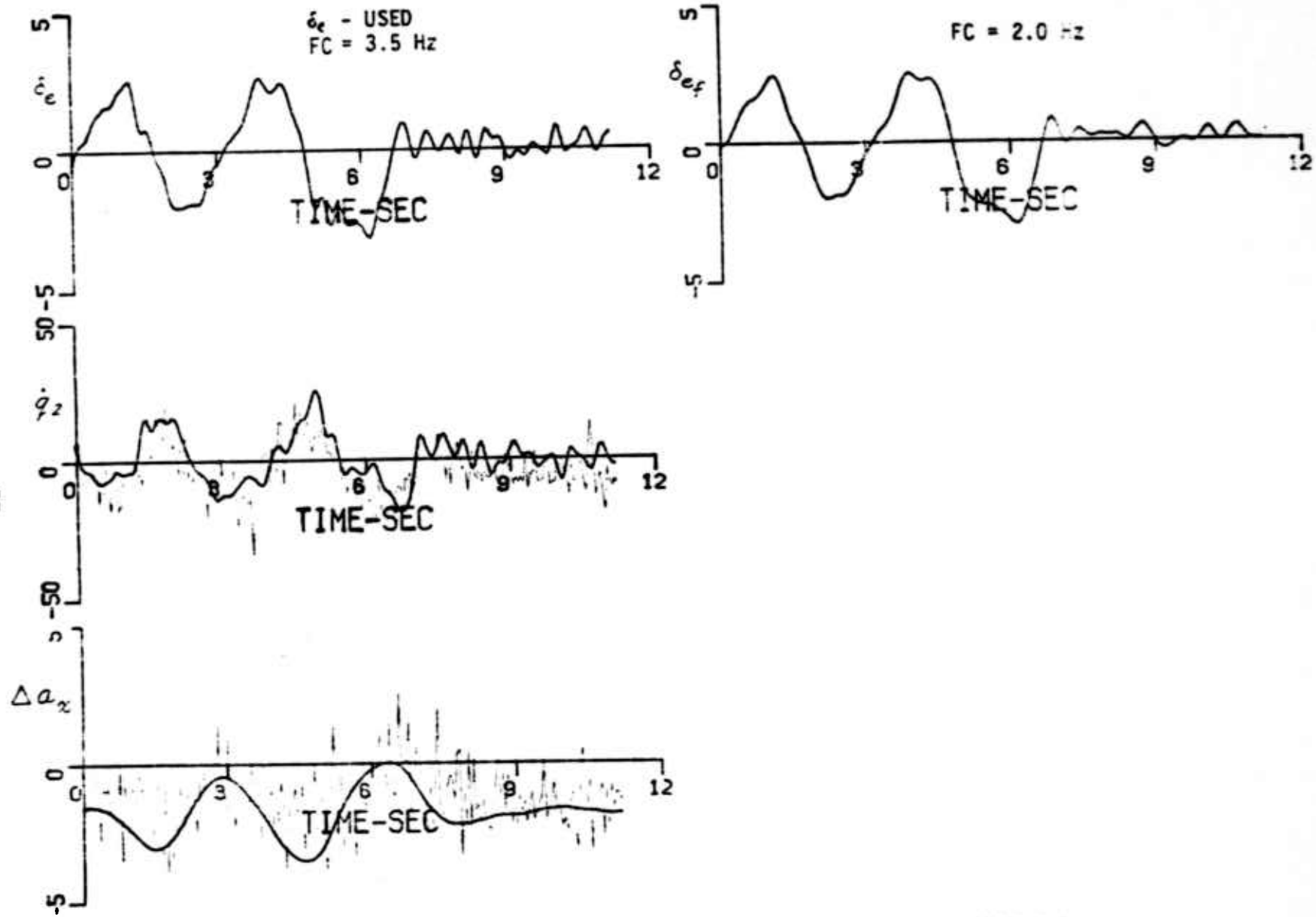

Figure 5a RESPONSE COMPARISONS WITH FLIGHT DATA - CASE 5-2

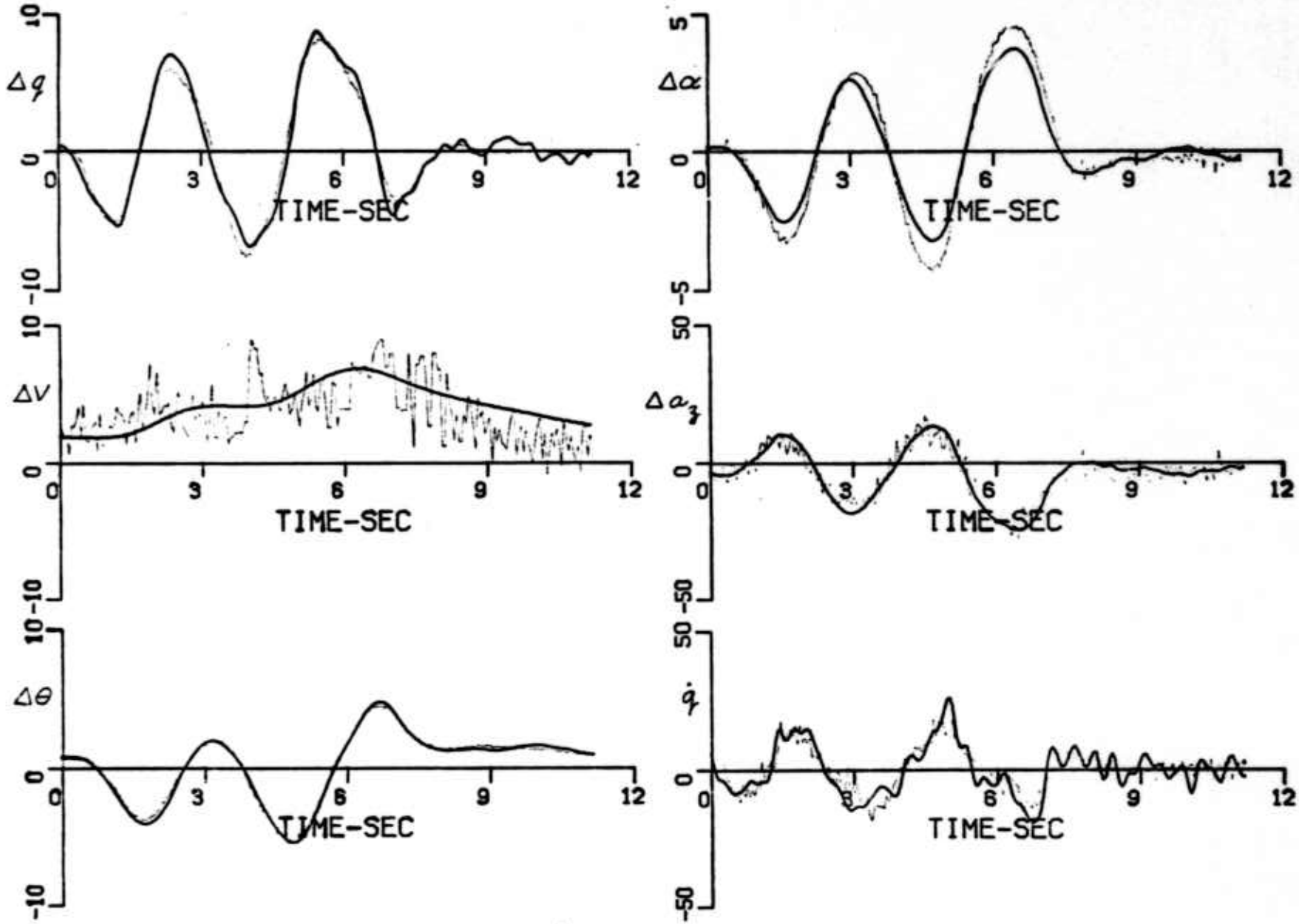

Figure 5a (cont'd) RESPONSE COMPARISONS WITH FLIGHT DATA - CASE 5-2

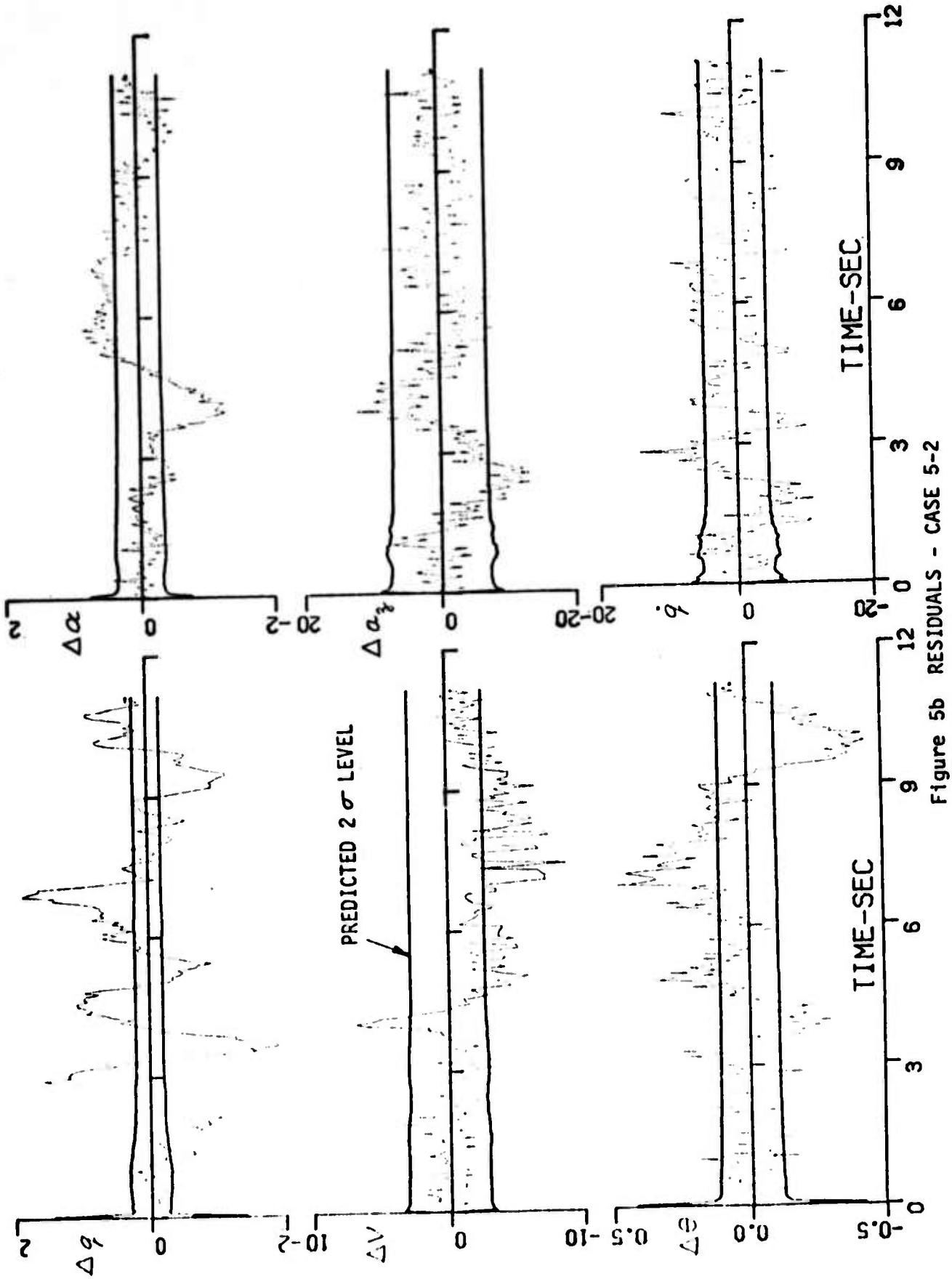

Figure 5b RESIDUALS - CASE 5-2

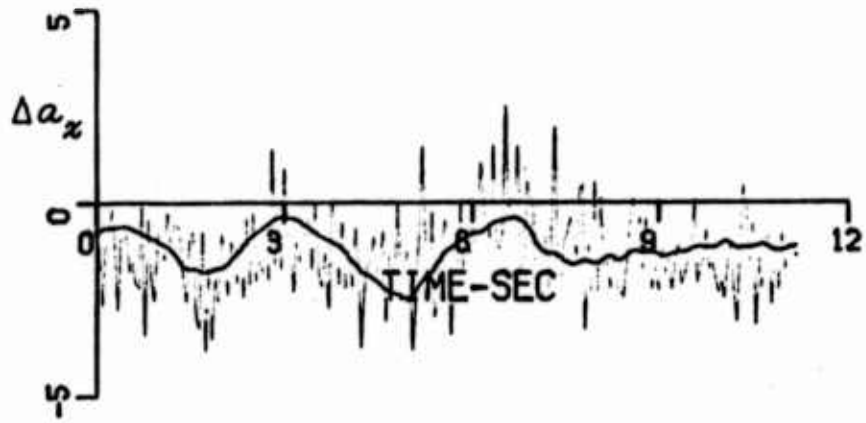

a. Response Comparisons with Δa_x - Case 5-1

Figure 6 RESPONSE COMPARISONS WITH PERTINENT MEASUREMENTS FOR CASES 5-1, 5-3 and 5-4

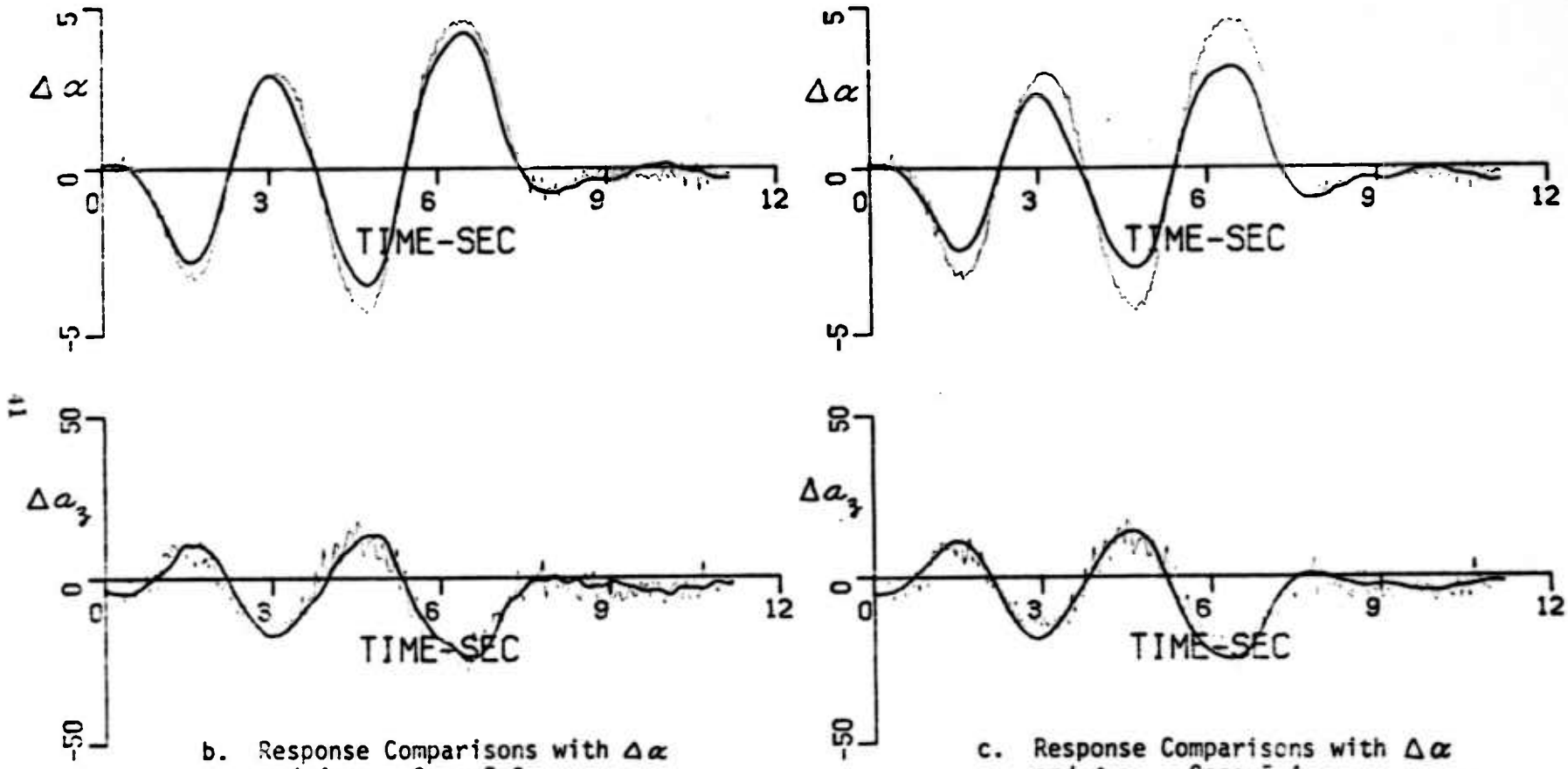

b. Response Comparisons with $\Delta\alpha$ and Δa_z - Case 5-3

c. Response Comparisons with $\Delta\alpha$ and Δa_z - Case 5-4

Figure 6 (cont'd) RESPONSE COMPARISONS WITH PERTINENT MEASUREMENTS FOR CASES 5-1, 5-3 AND 5-4

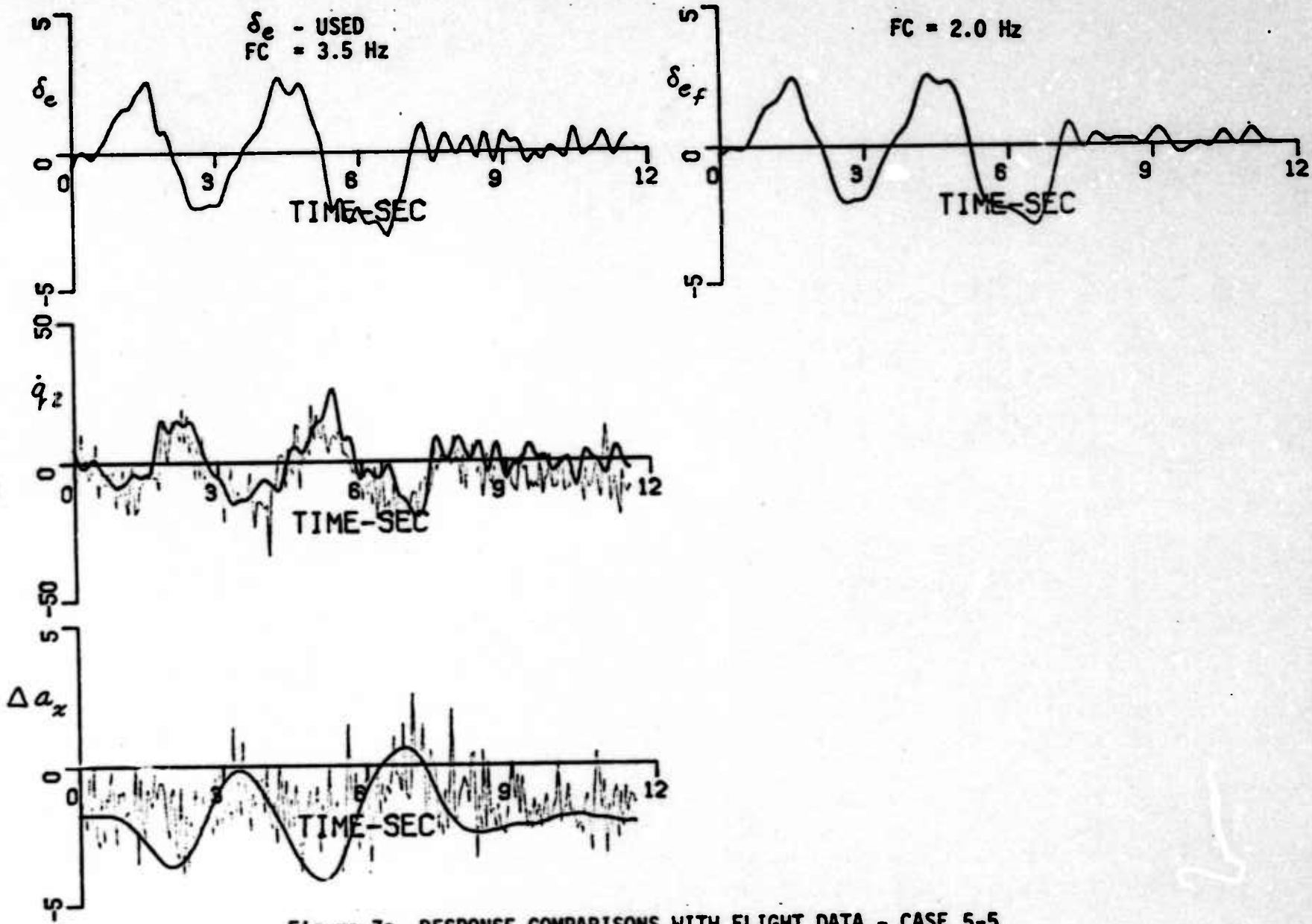

Figure 7a RESPONSE COMPARISONS WITH FLIGHT DATA - CASE 5-5

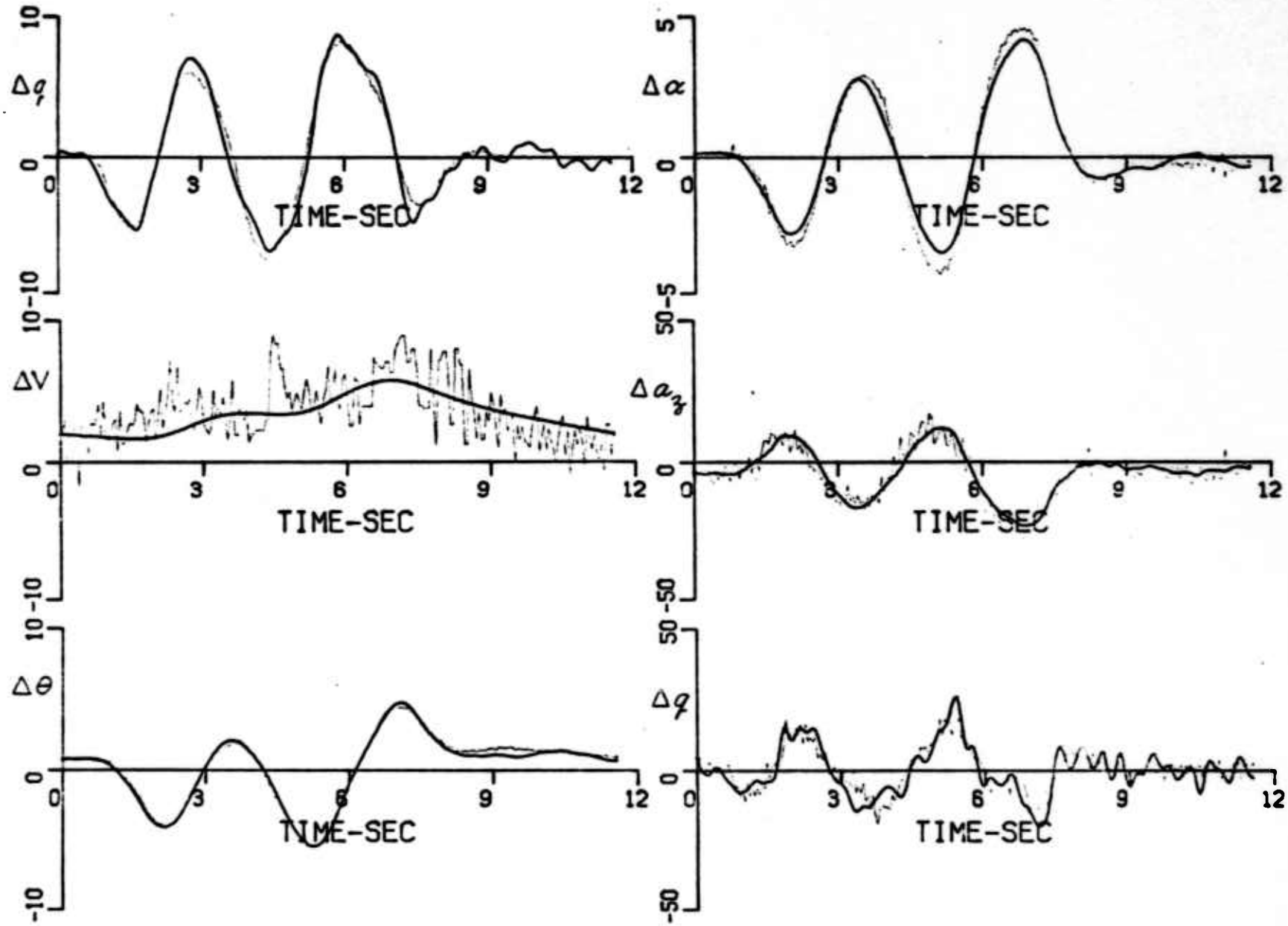

Figure 7a (cont'd) RESPONSE COMPARISONS WITH FLIGHT DATA - CASE 5-5

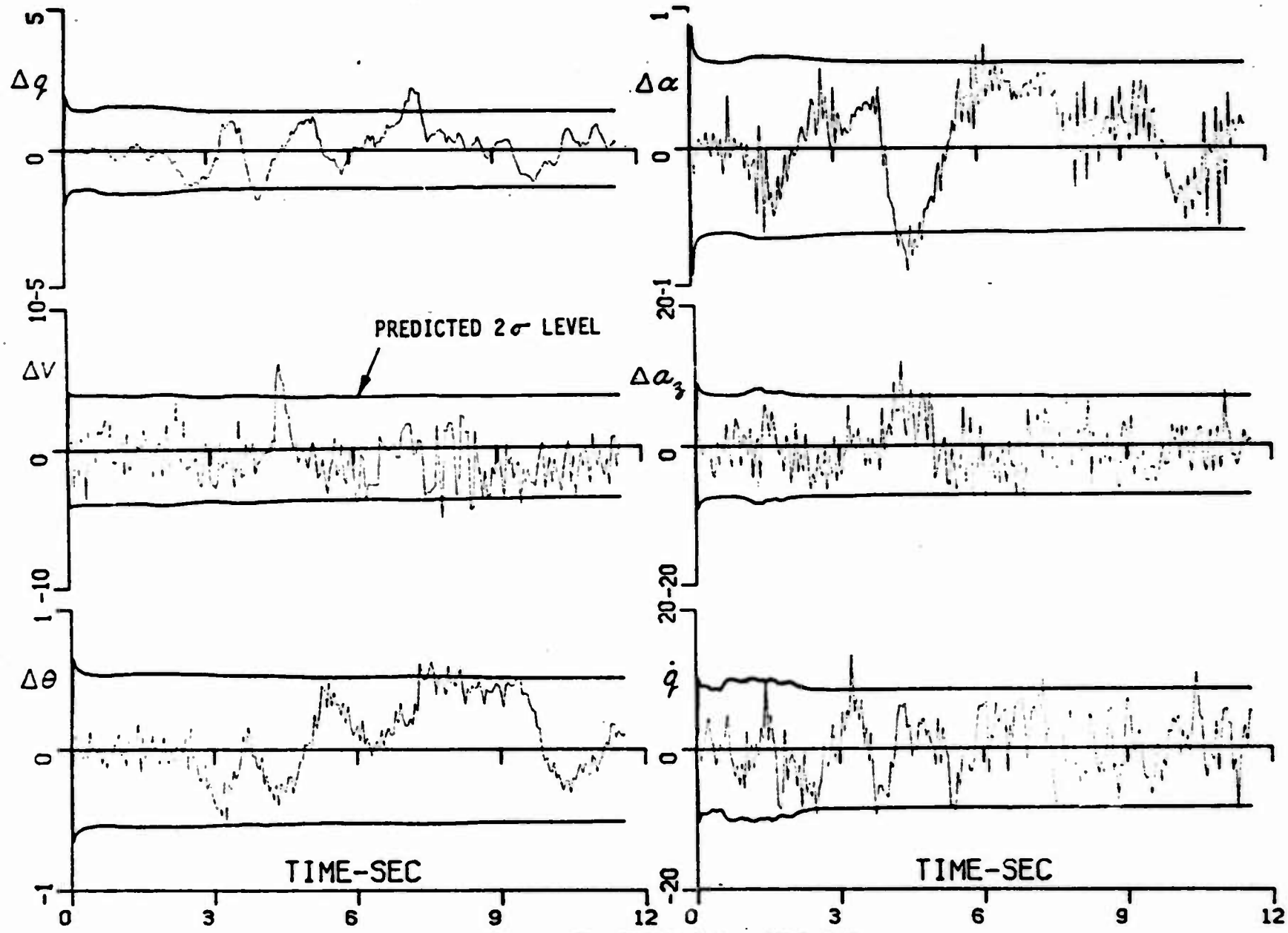

Figure 7b RESIDUALS - CASE 5-5

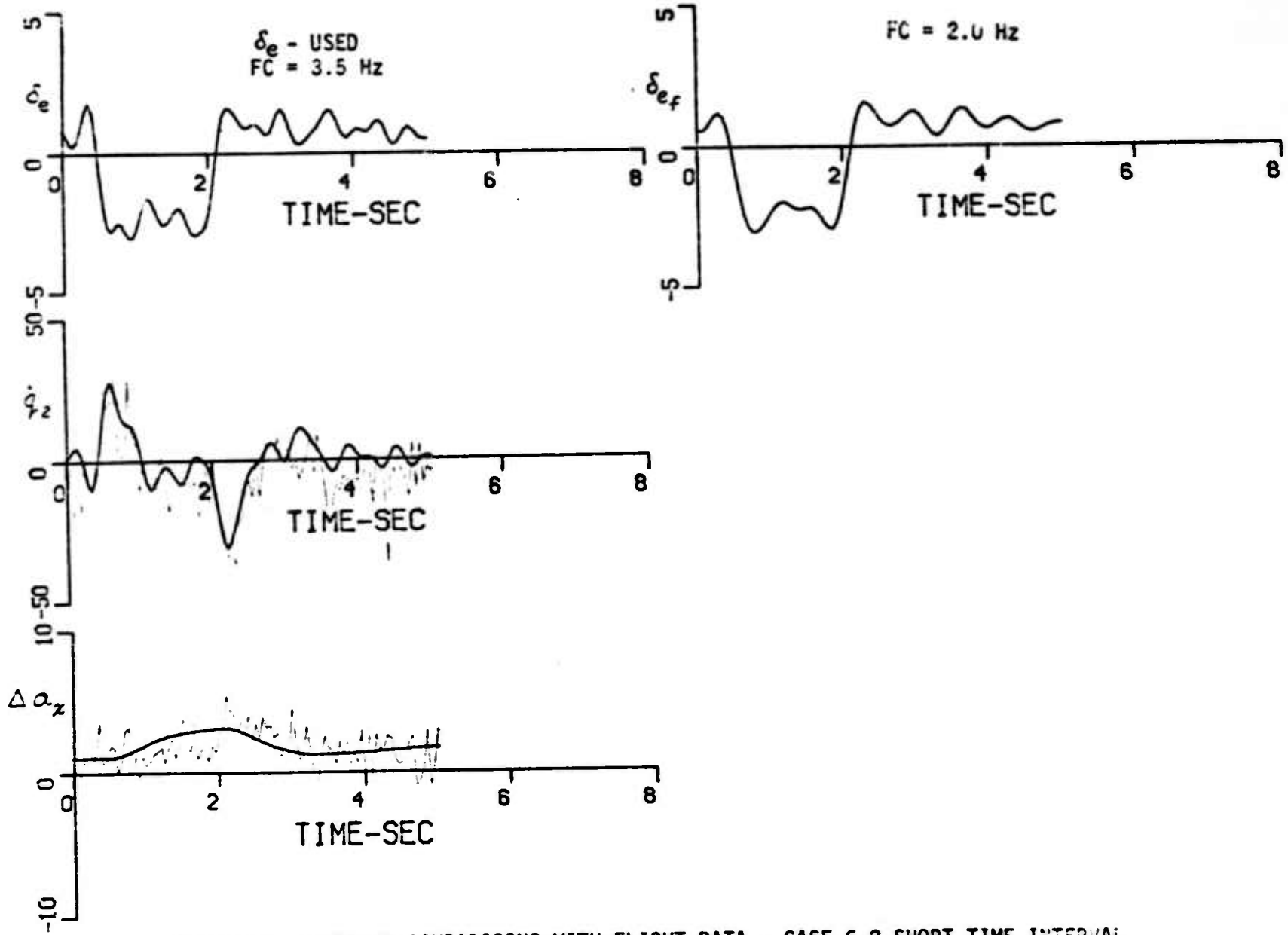

Figure 8 RESPONSE COMPARISONS WITH FLIGHT DATA - CASE 6-2 SHORT TIME INTERVAL

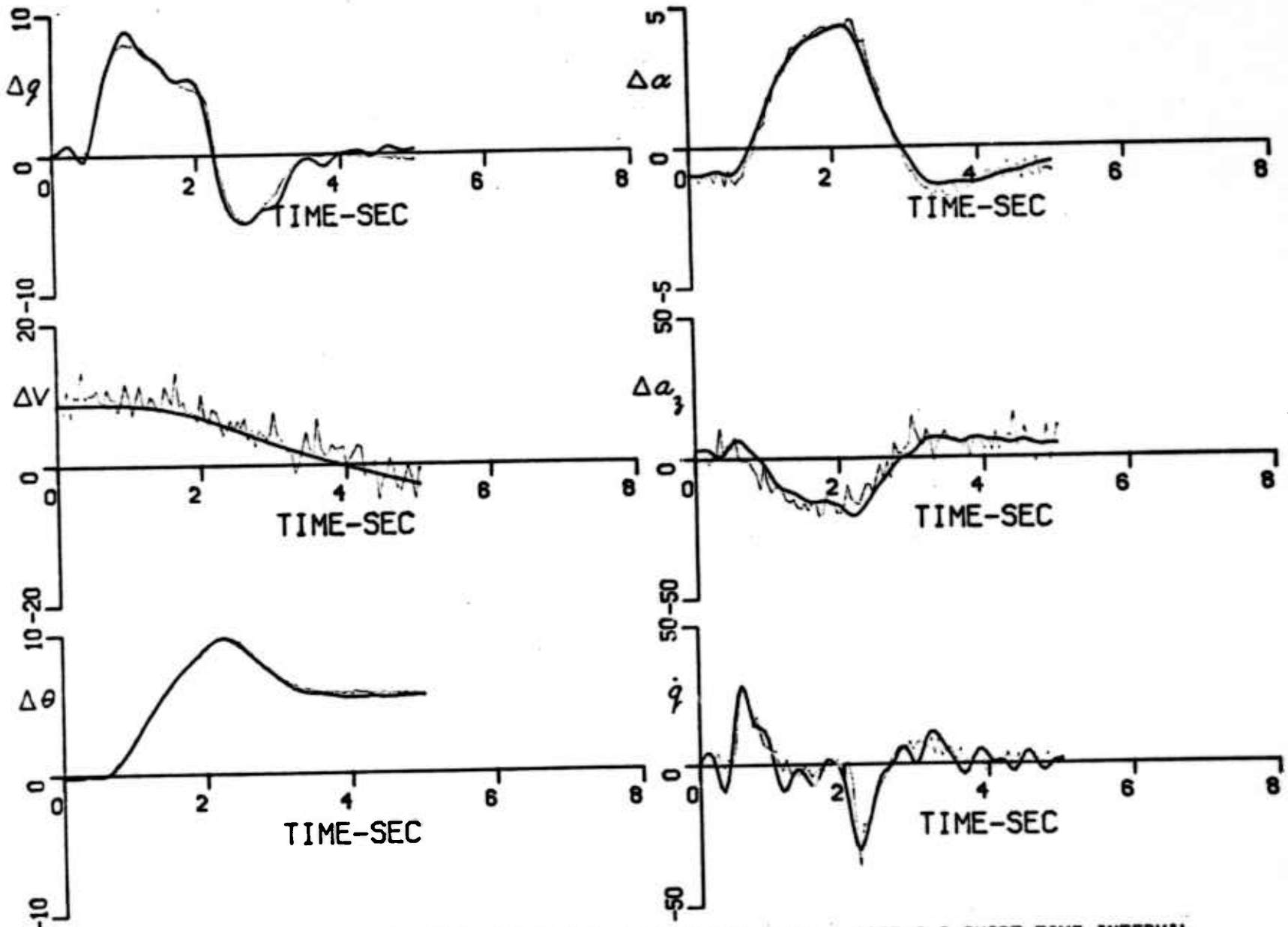

Figure 8 (cont'd) RESPONSE COMPARISONS WITH FLIGHT DATA - CASE 6-2, SHORT TIME INTERVAL

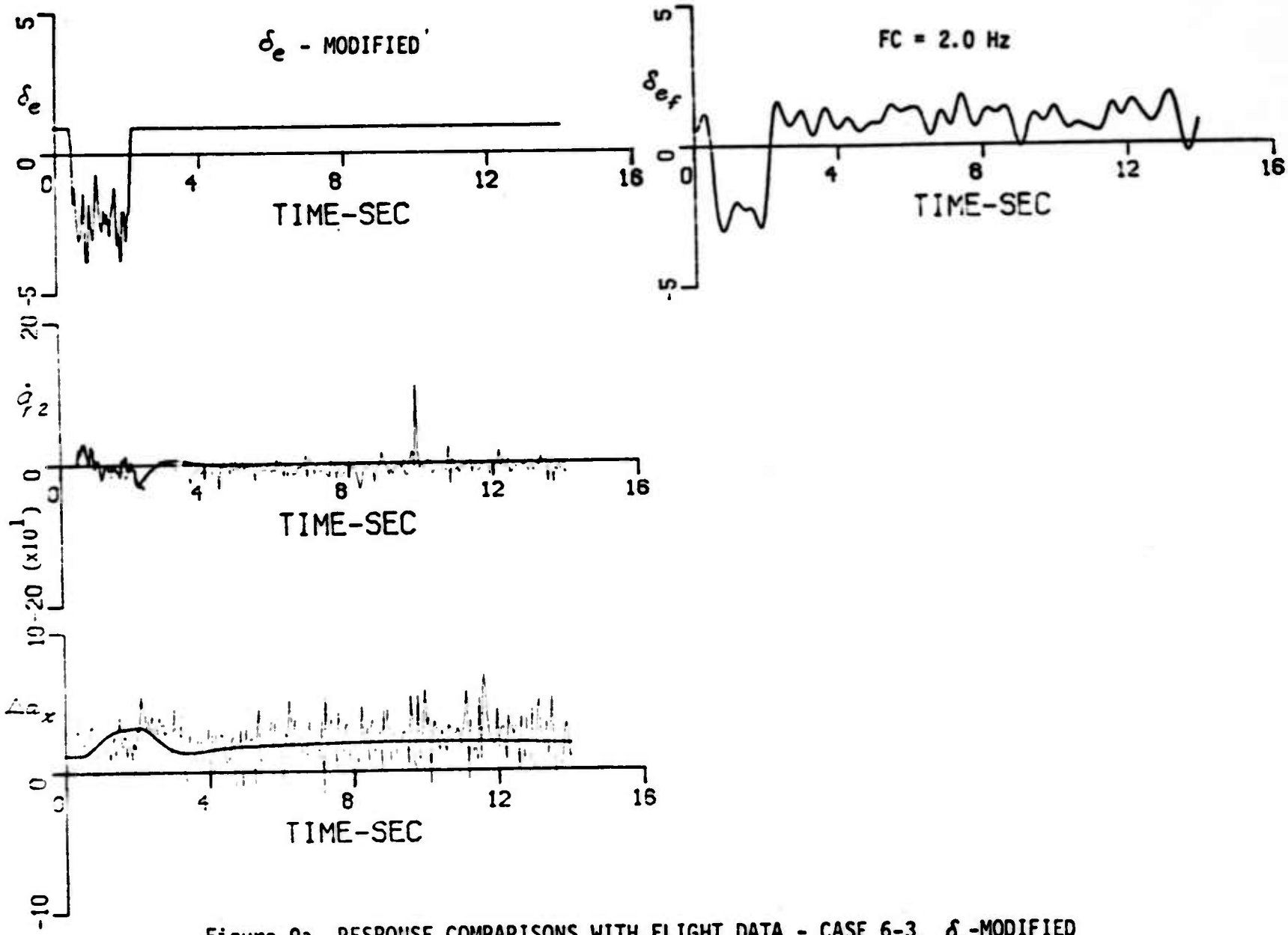

Figure 9a RESPONSE COMPARISONS WITH FLIGHT DATA - CASE 6-3, δ_e-MODIFIED

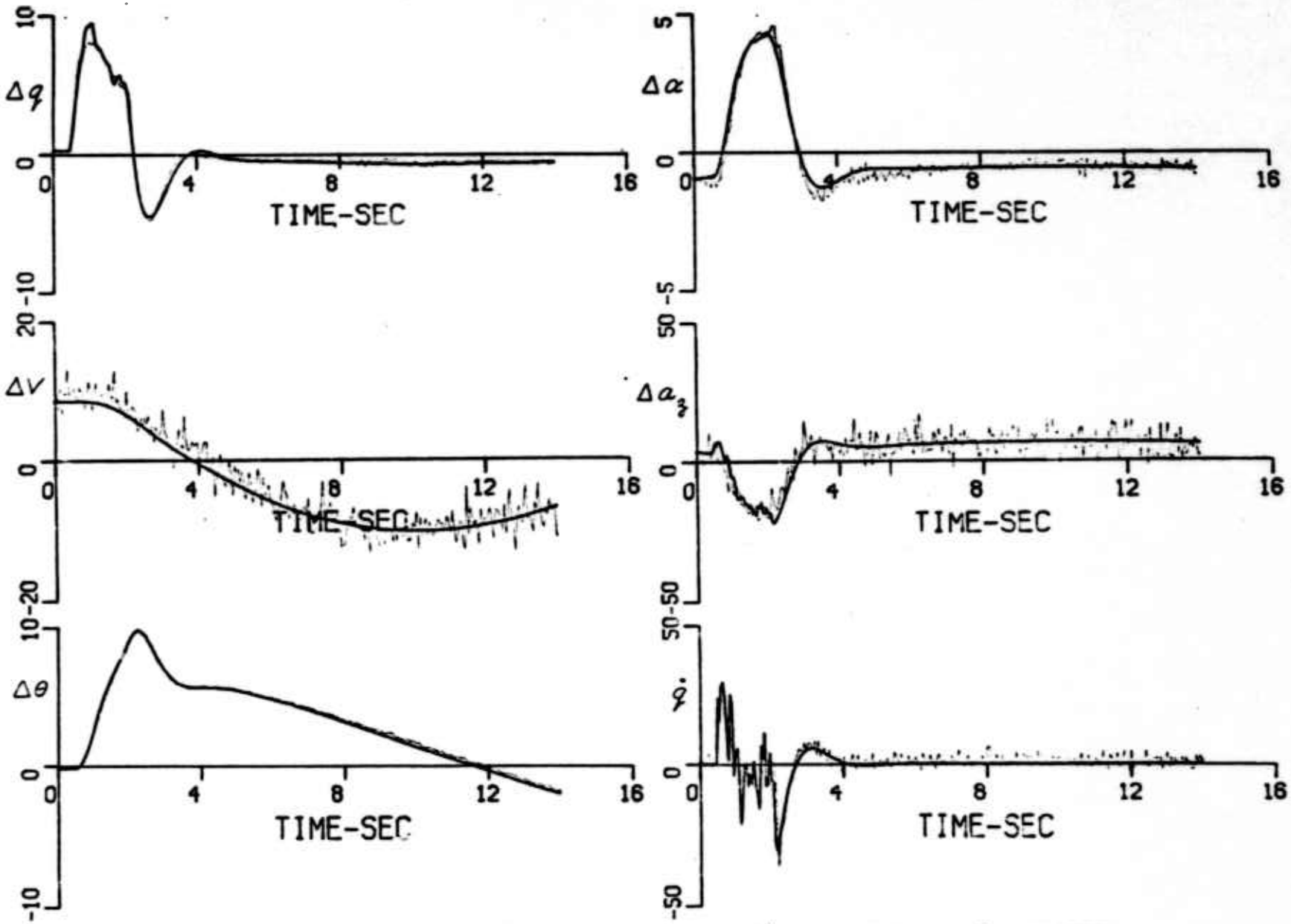

Figure 9a (cont'd) RESPONSE COMPARISONS WITH FLIGHT DATA - CASE 6-3, δ_e -MODIFIED

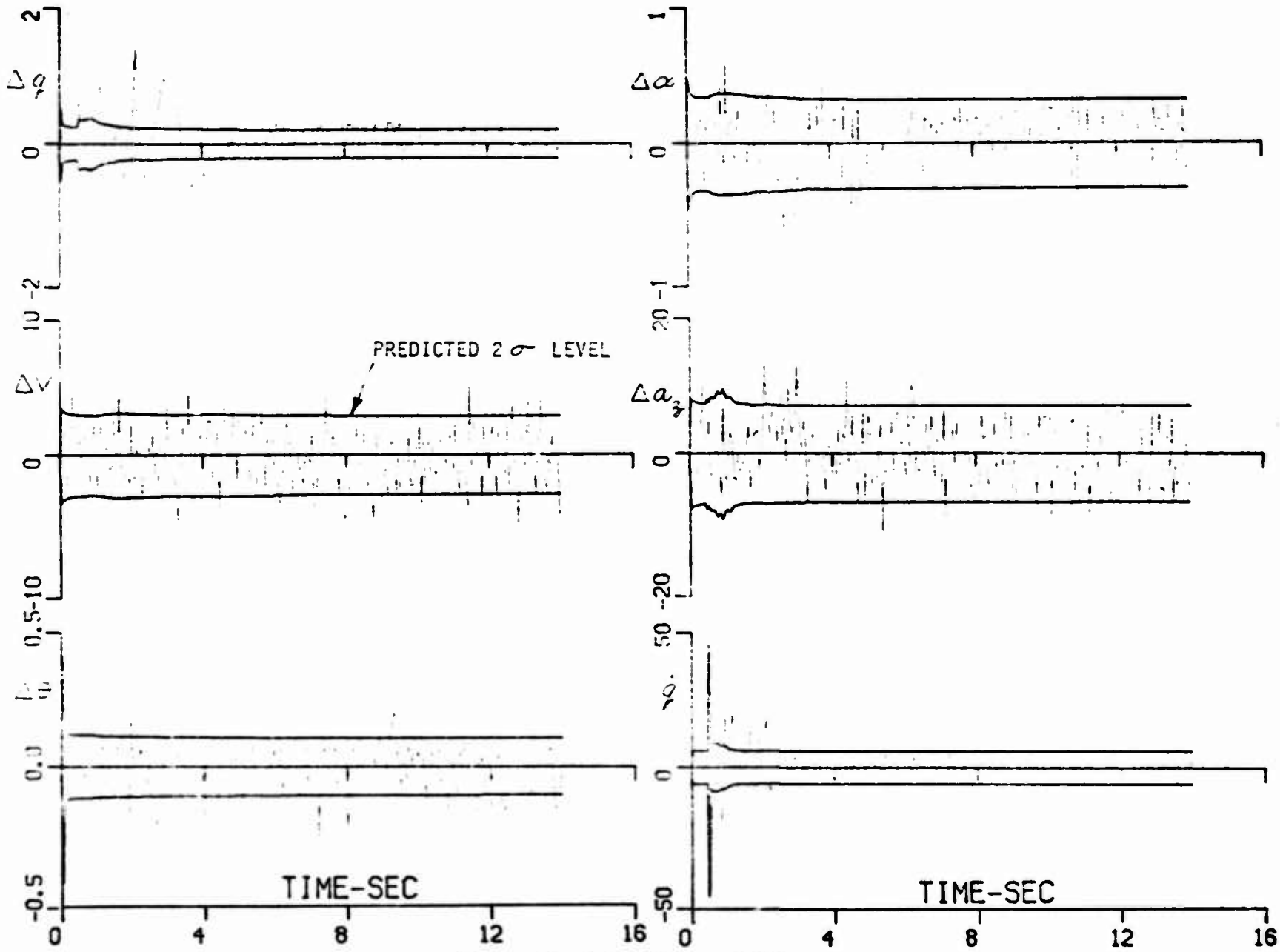

Figure 9b RESIDUALS - CASE 6-3

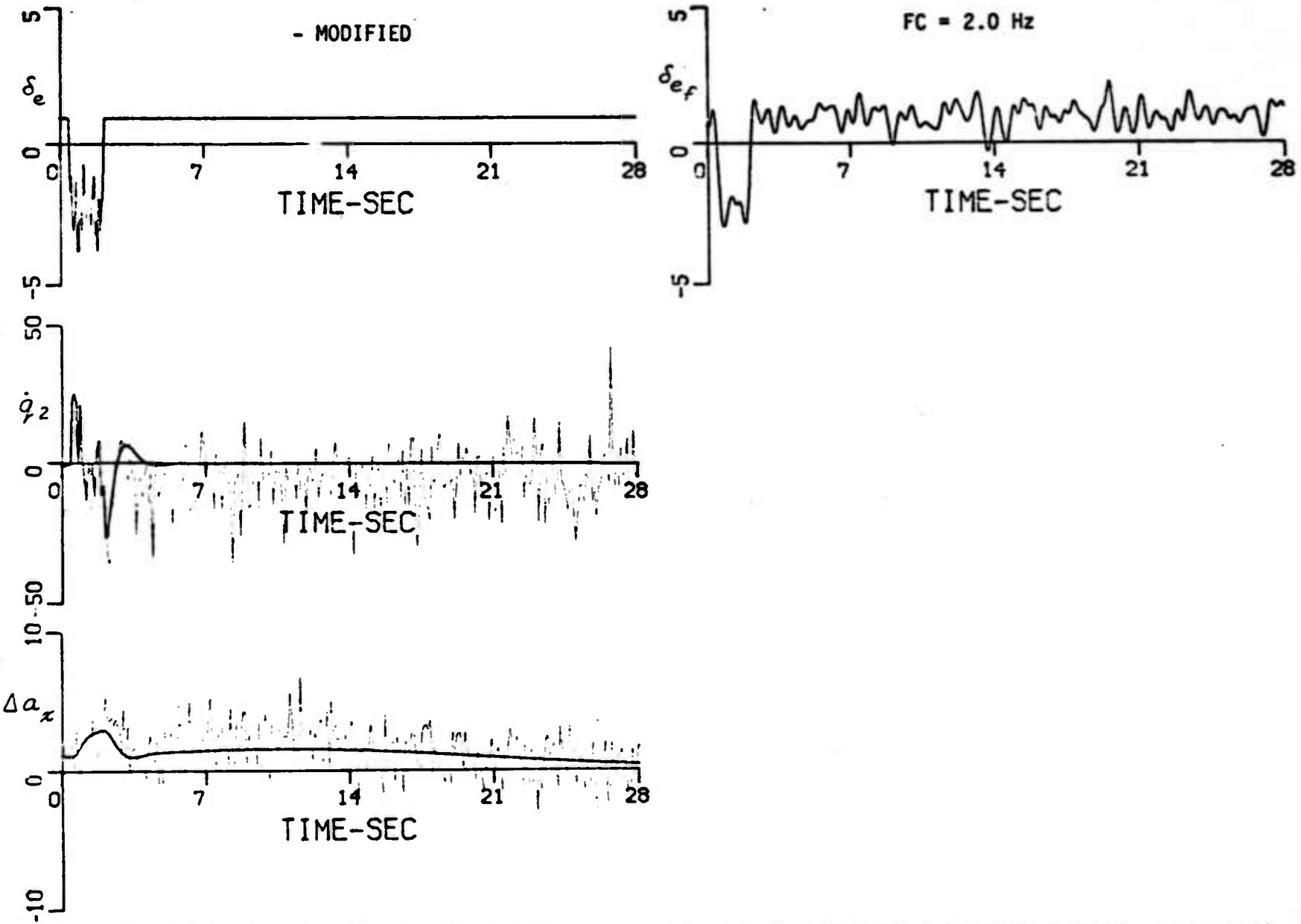

Figure 10 RESPONSE COMPARISONS WITH FLIGHT DATA - CASE 6-5, δ_e -MODIFIED, LONG TIME INTERVAL ($\Delta t = 0.1$)

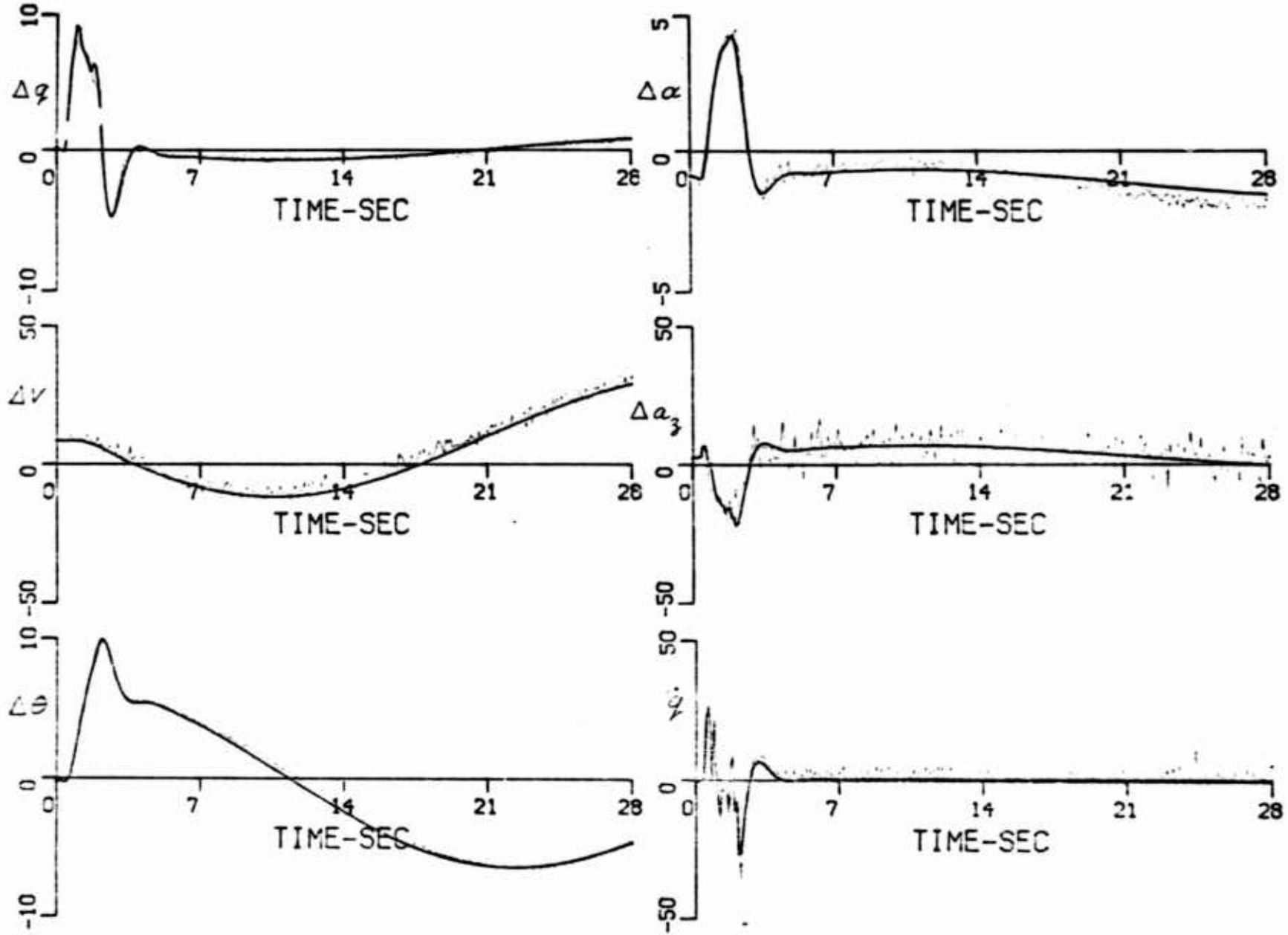

Figure 10 (cont'd) RESPONSE COMPARISONS WITH FLIGHT DATA - CASE 6-5, δ_e MODIFIED, LONG TIME INTERVAL ($\Delta t = 0.1$)

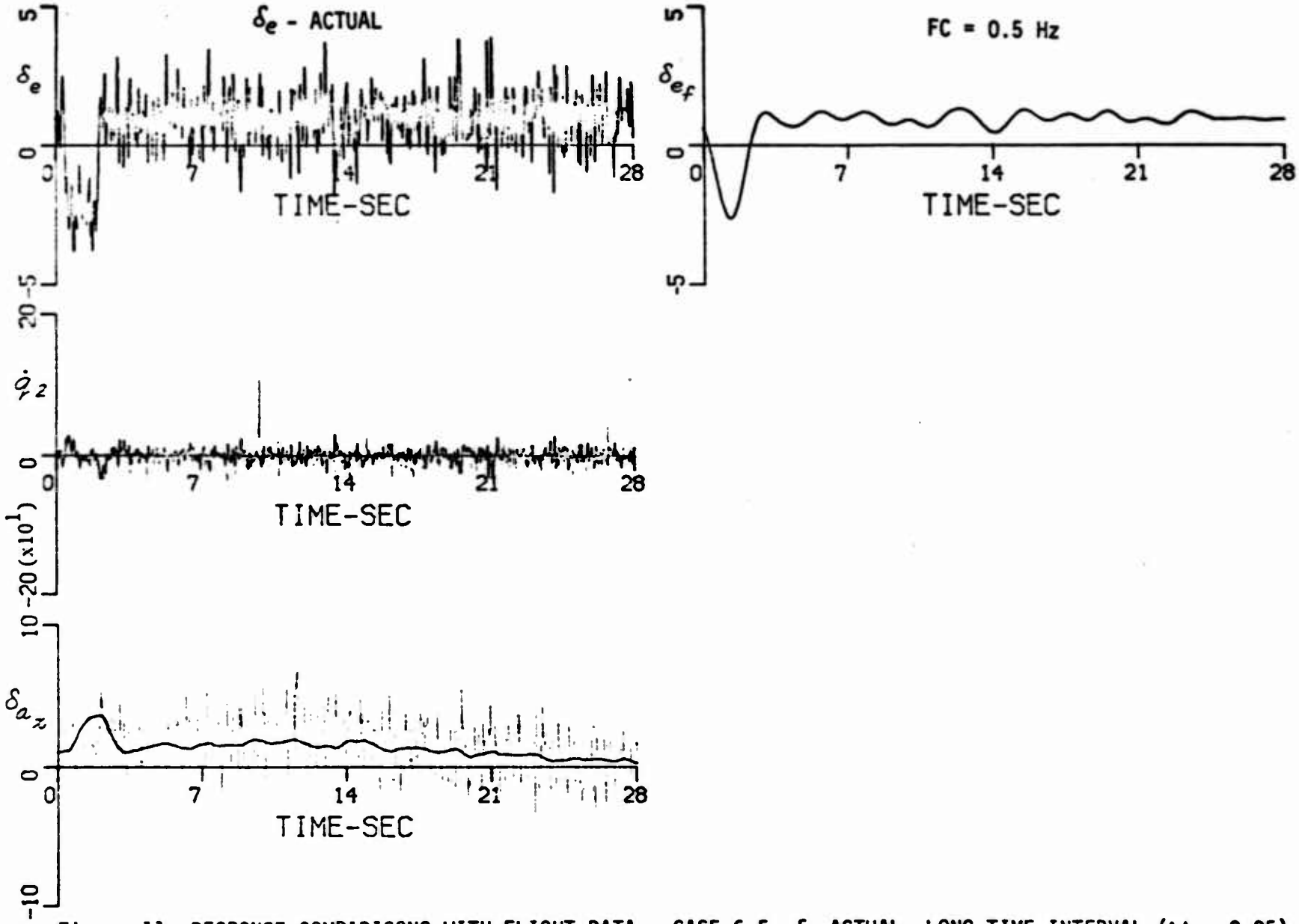

Figure 11 RESPONSE COMPARISONS WITH FLIGHT DATA - CASE 6-5, δ_e ACTUAL, LONG TIME INTERVAL (Δt = 0.05)

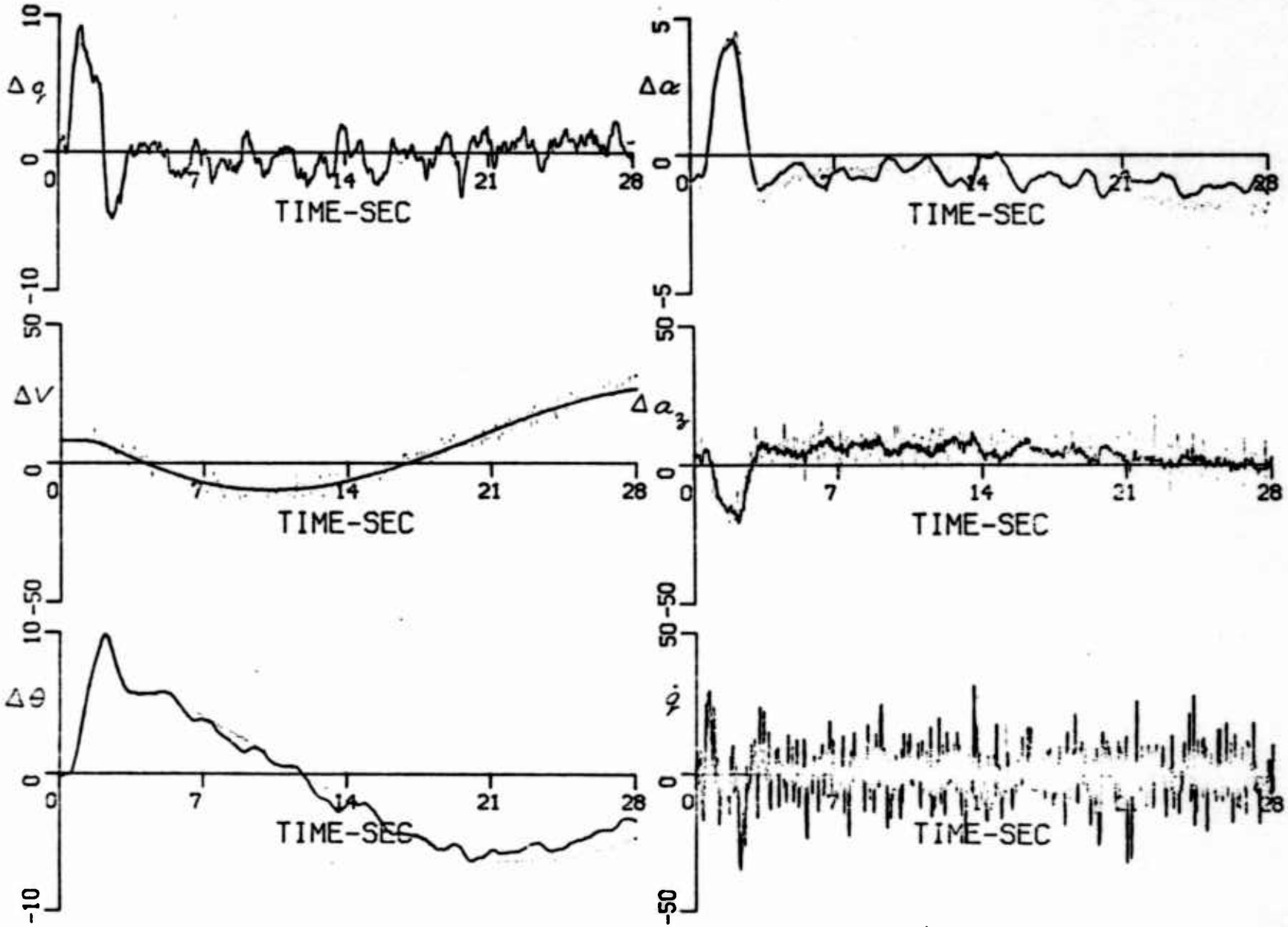

Figure 11 (cont'd) RESPONSE COMPARISONS WITH FLIGHT DATA - CASE 6-5, δ_e ACTUAL, LONG TIME INTERVAL ($\Delta t = 0.05$)

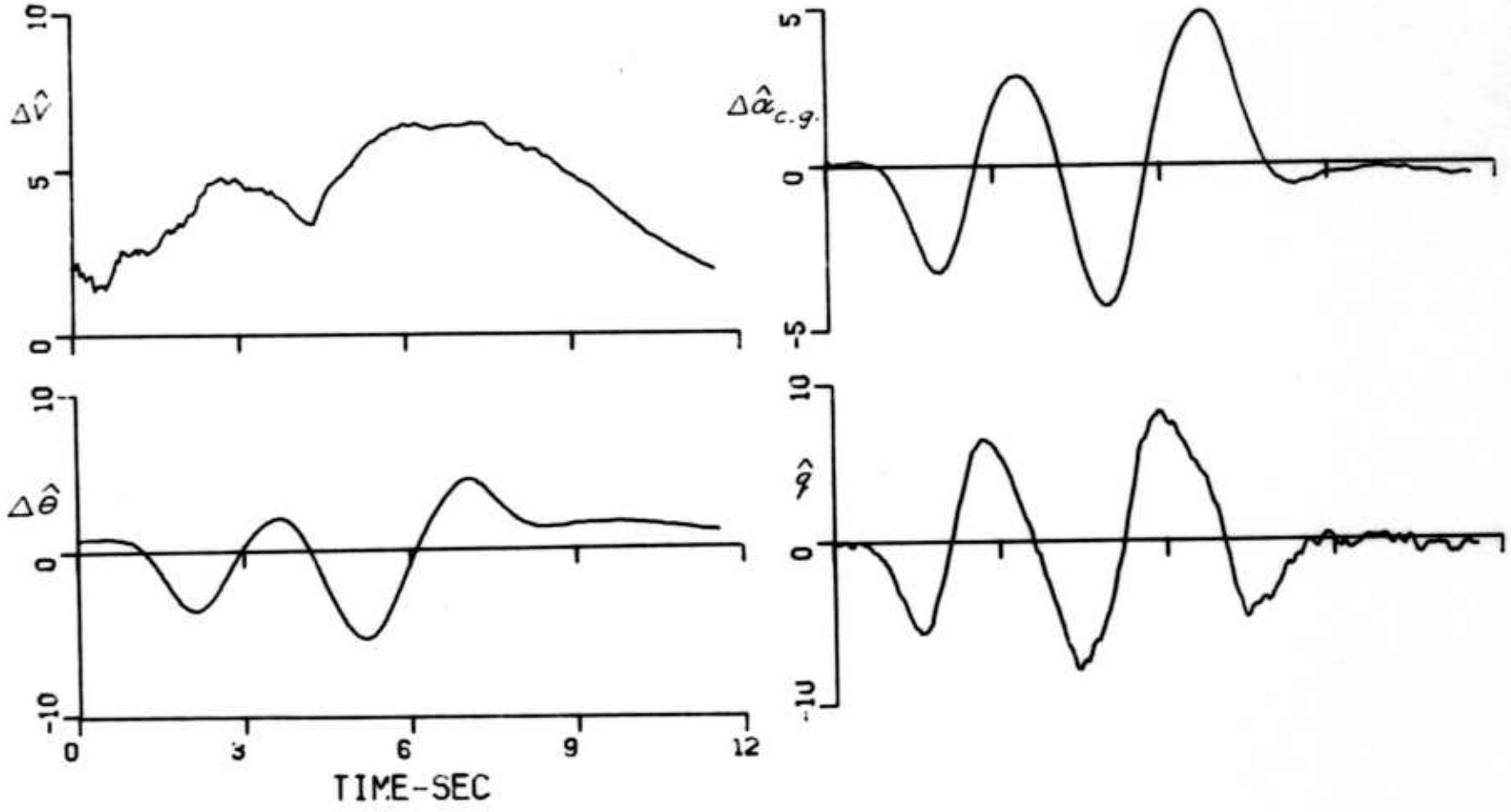

Figure 12 TIME HISTORIES OF STATE ESTIMATES AND RESIDUALS - CASE 5-6 ($Q \neq 0$ AND δ_e UNFILTERED)

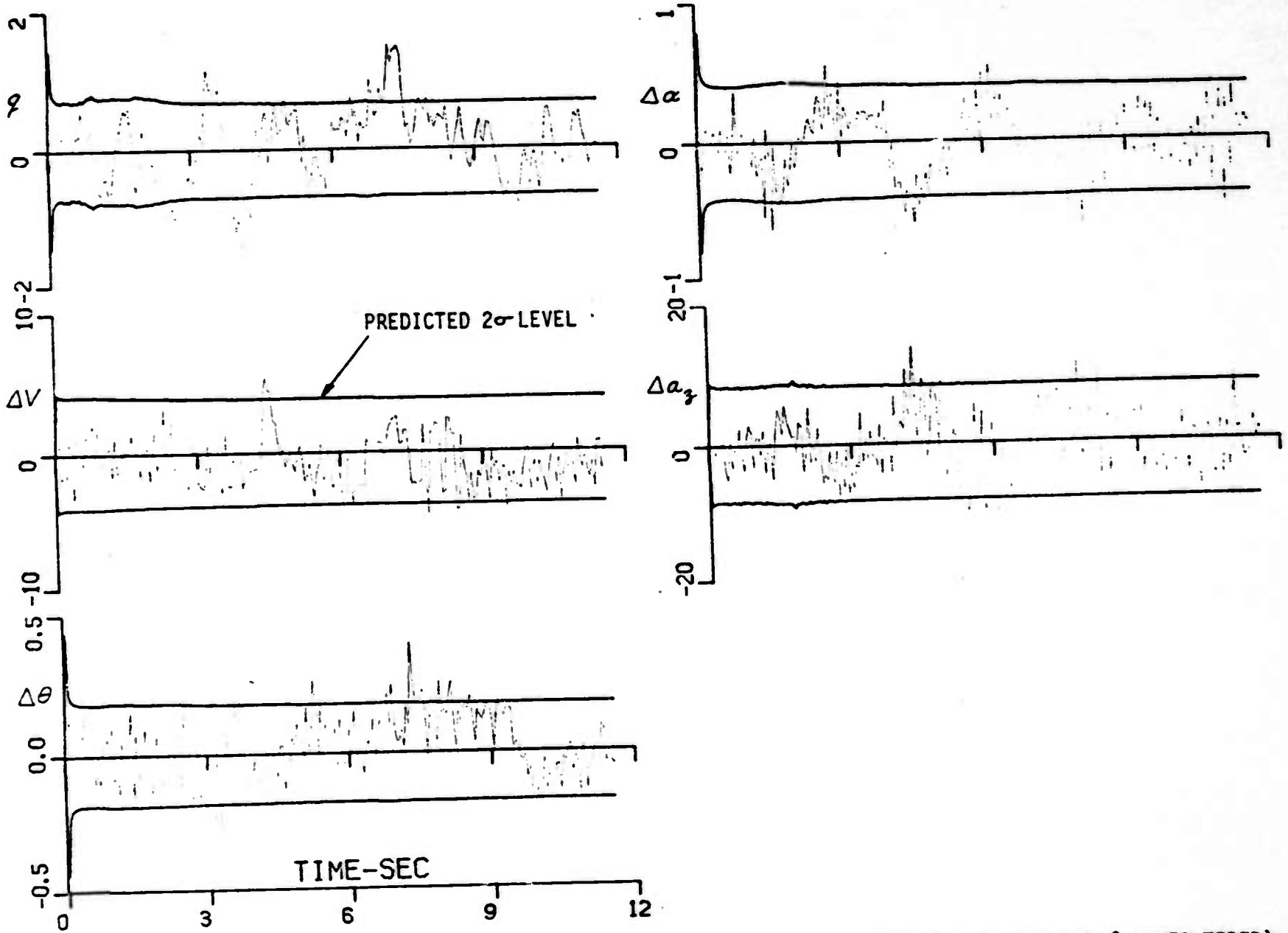

Figure 12 (cont'd) TIME HISTORIES OF STATE ESTIMATES AND RESIDUALS - CASE 5-6 ($Q \neq 0$ AND δ_e UNFILTERED)

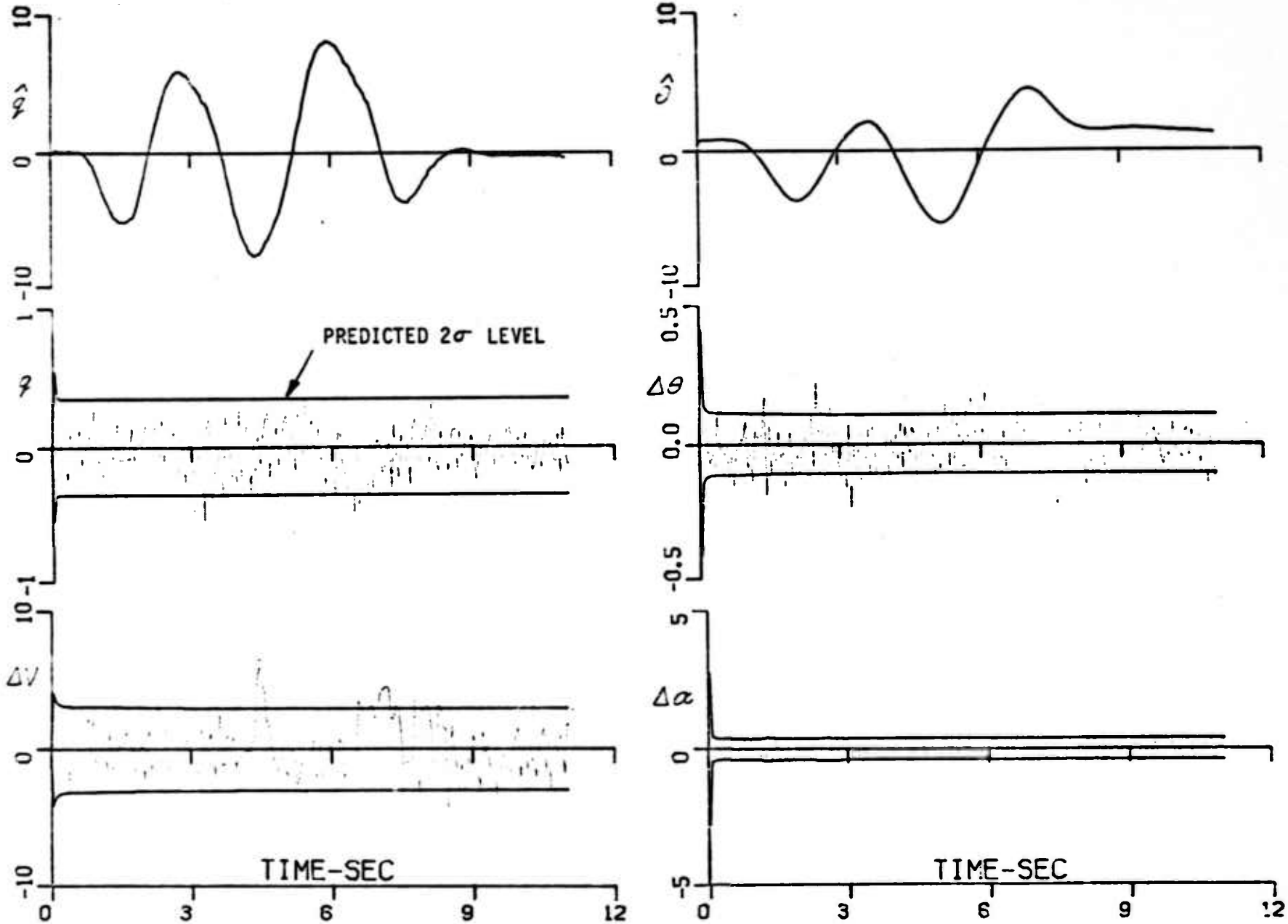

Figure 13 TIME HISTORIES OF RESIDUALS AND STATE ESTIMATES FOR INSTRUMENTATION CONSISTENCY RELATIONSHIPS - RECORD 5

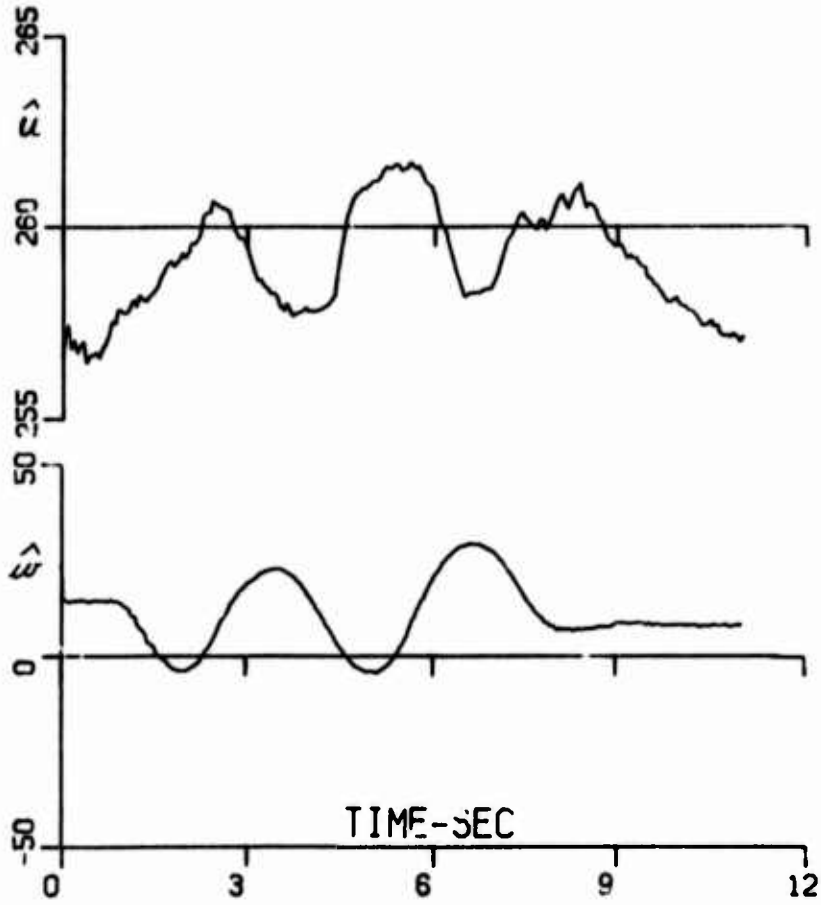

Figure 13 (cont'd) TIME HISTORIES OF RESIDUALS AND STATE ESTIMATES FOR INSTRUMENTATION CONSISTENCY RELATIONSHIPS - RECORD 5

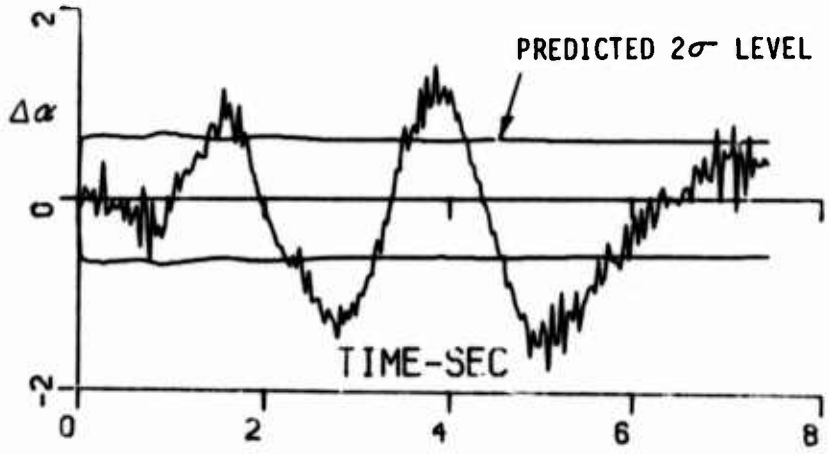

Figure 14 RESIDUAL FOR $\Delta\alpha$ WITHOUT SCALE FACTOR - RECORD 5

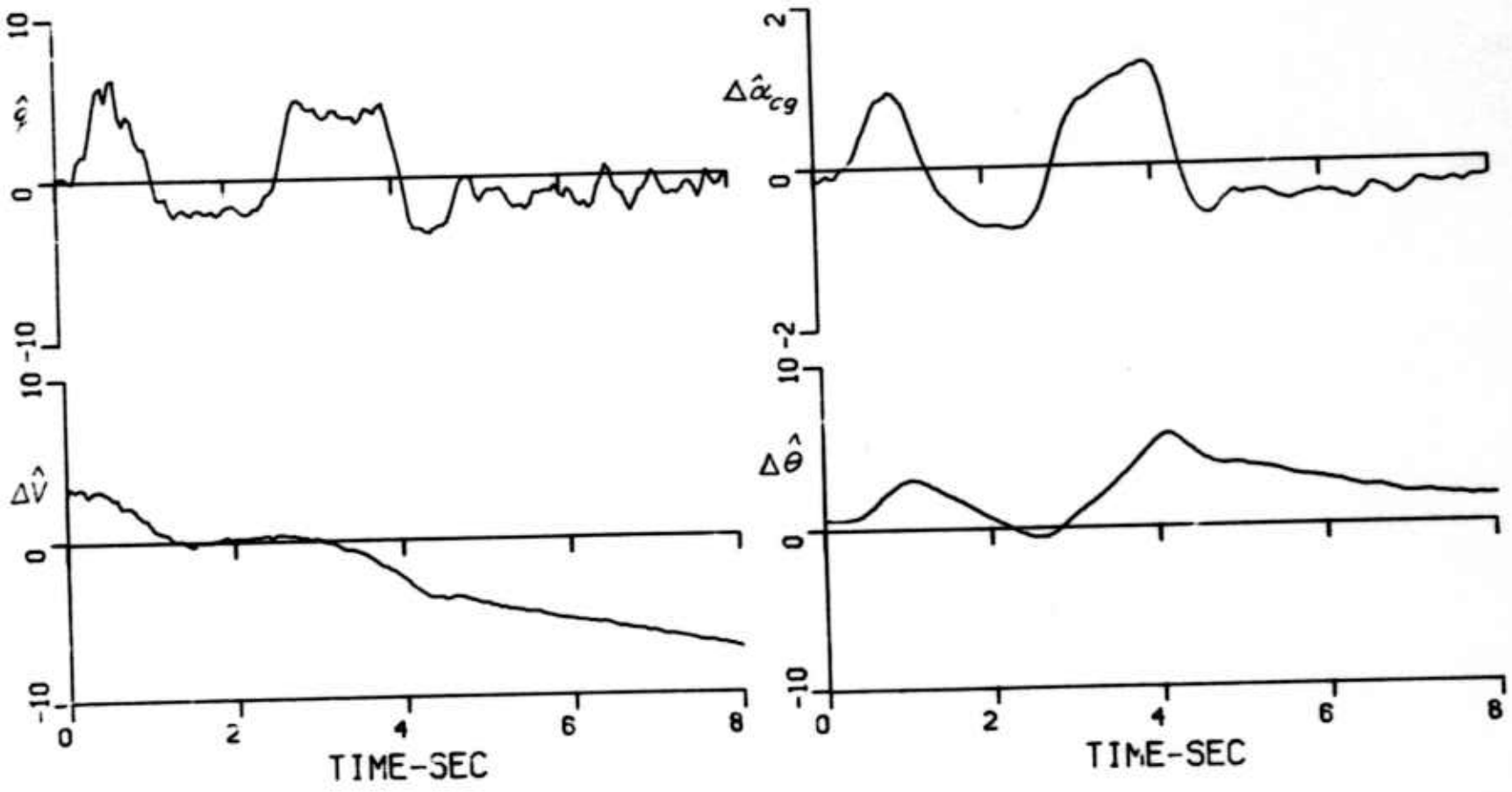

Figure 15 TIME HISTORIES OF STATE ESTIMATES AND RESIDUALS - RECORD 13-1 ($Q \neq 0$ AND δ_e UNFILTERED)

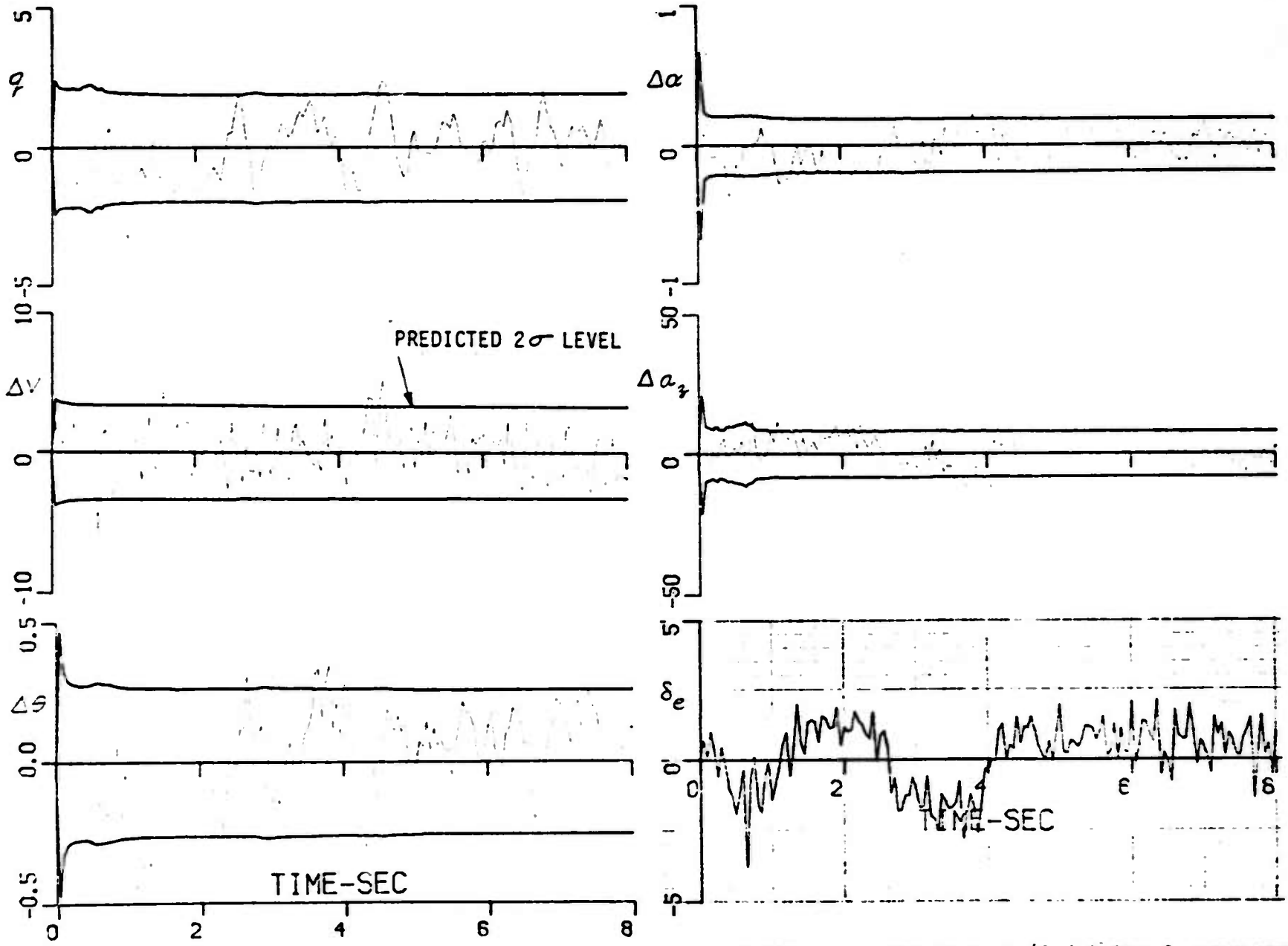

Figure 15 (cont'd) TIME HISTORIES OF STATE ESTIMATES AND RESIDUALS – RECORD 13-1 ($Q \neq 0$ AND δ_e UNFILTERED)

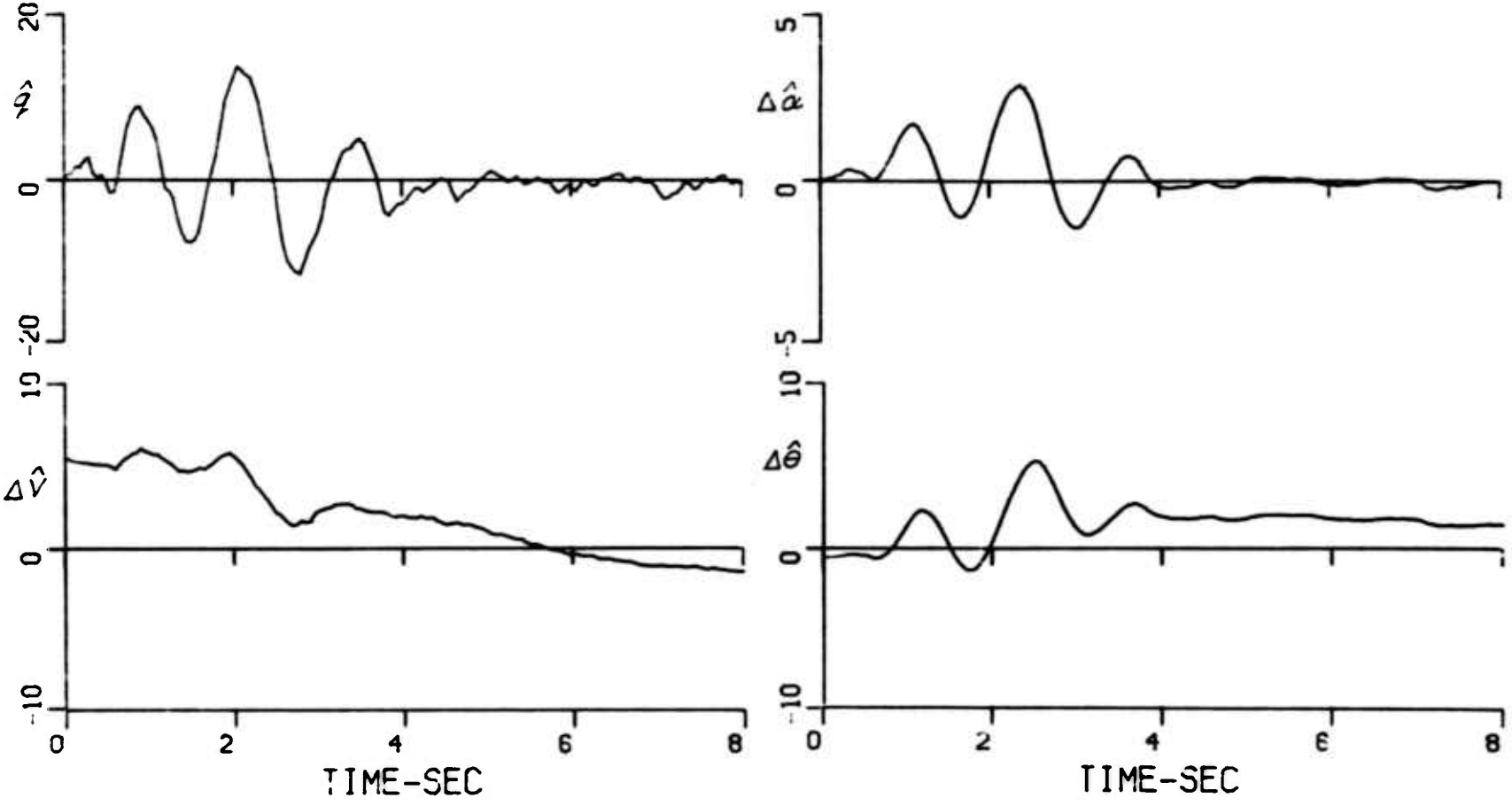

Figure 16 TIME HISTORIES OF STATE ESTIMATES AND RESIDUALS - RECORD 18-1 ($Q \neq 0$ AND δ_e UNFILTERED)

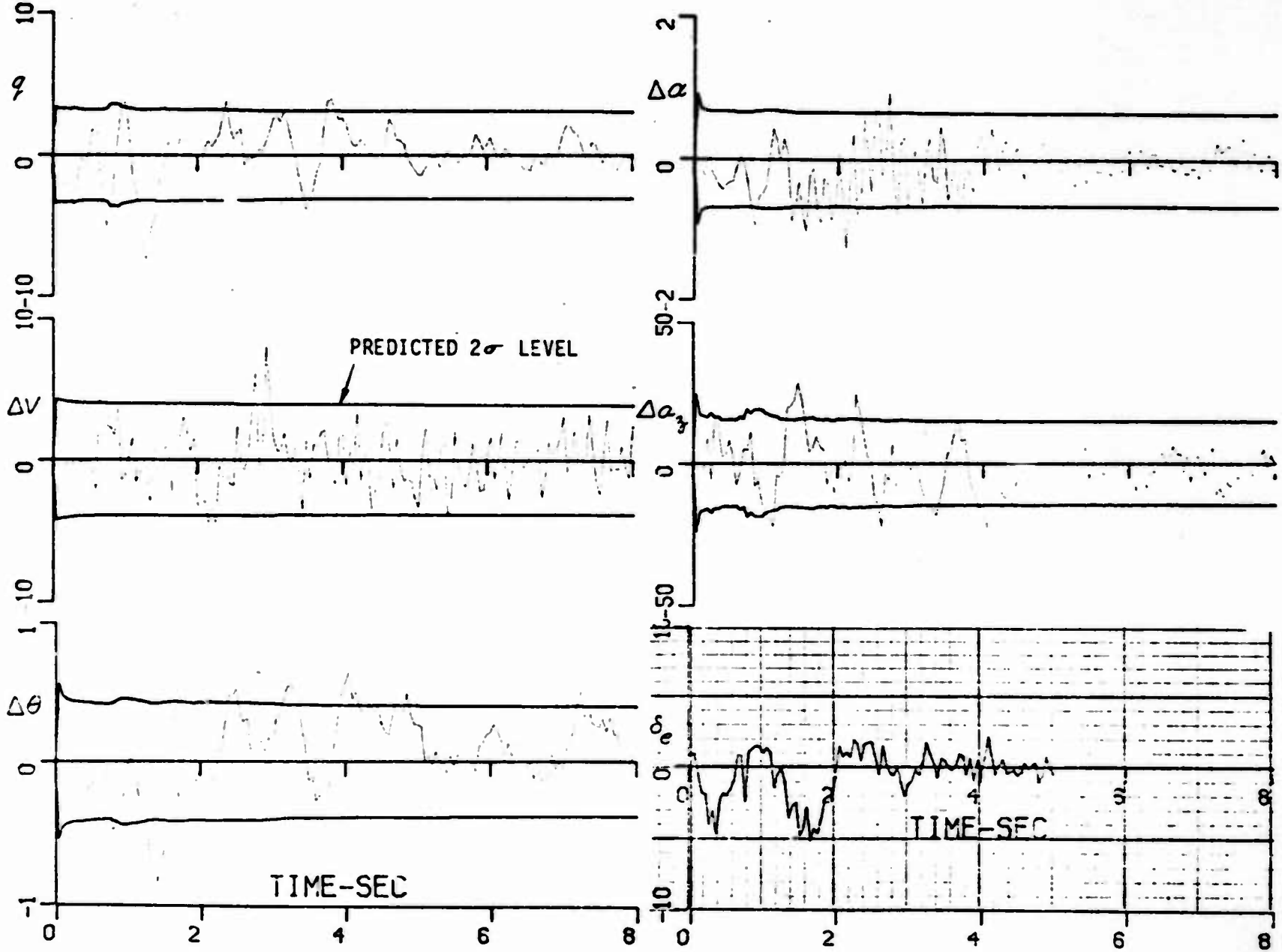

Figure 16 (cont'd) TIME HISTORIES OF STATE ESTIMATES AND RESIDUALS - RECORD 18-1 ($Q \neq 0$ AND δ_e UNFILTERED)

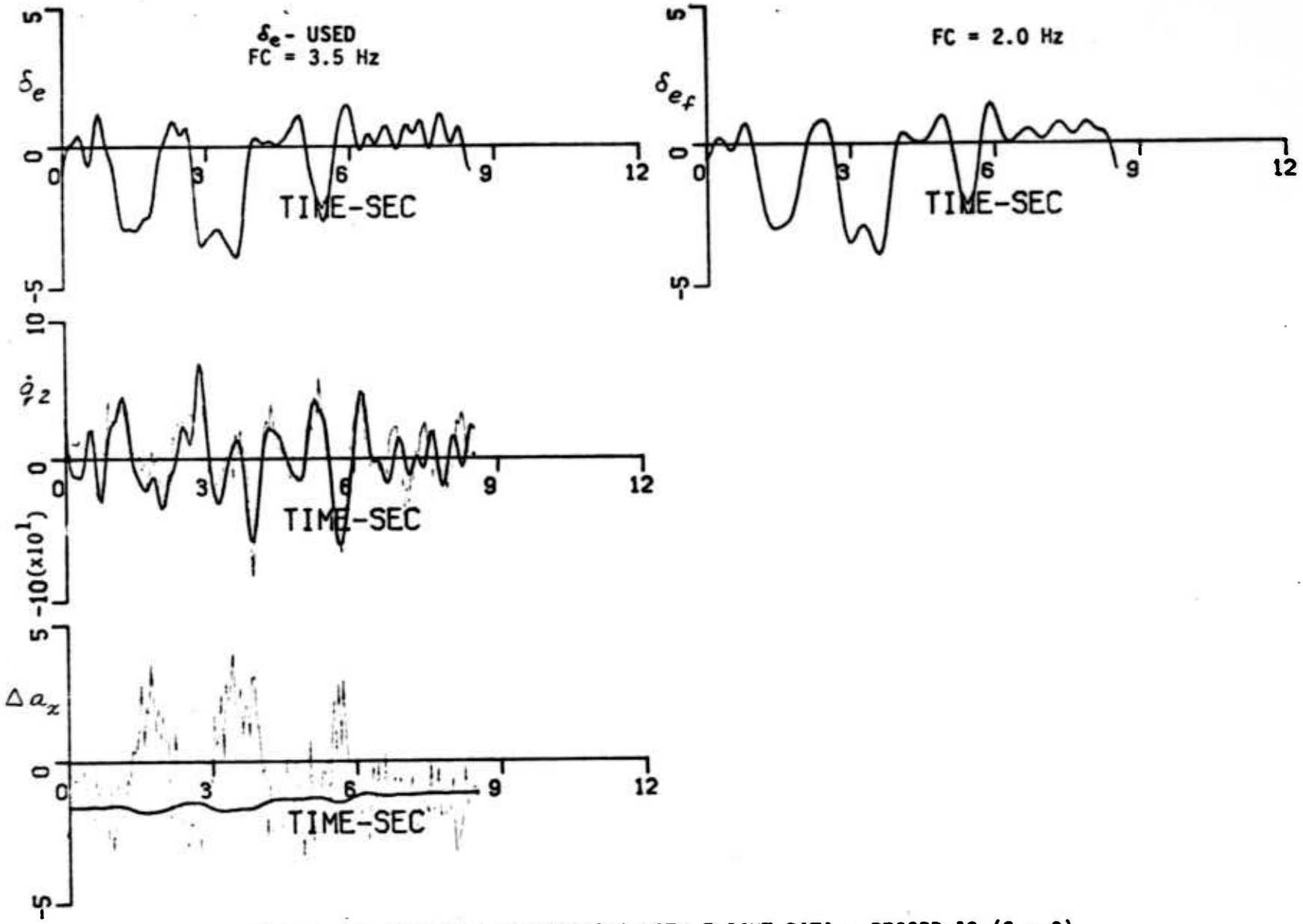

Figure 17 RESPONSE COMPARISONS WITH FLIGHT DATA - RECORD 19 (Q = 0)

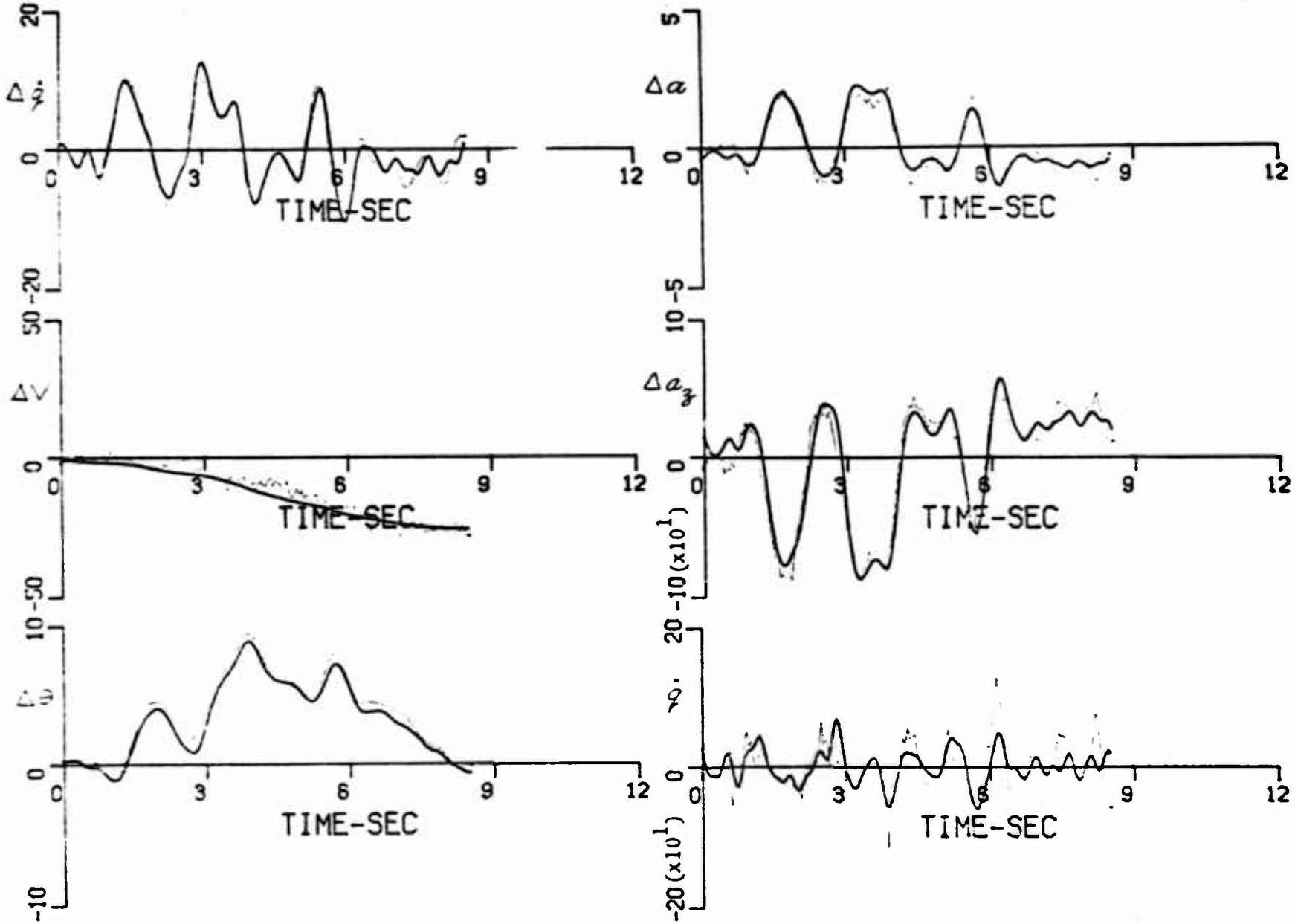

Figure 17 (cont'd) RESPONSE COMPARISONS TO FLIGHT DATA - RECORD 19 (Q = 0)

TABLE 1

MATHEMATICAL MODELS

Longitudinal Equations of Motion:

$$\begin{bmatrix} \dot{\theta} \\ \dot{V} \\ \dot{q} \\ \dot{\alpha} \end{bmatrix} = \begin{bmatrix} 0 & 0 & 1 & 0 \\ X_\theta & X_V & X_q & X_\alpha + \frac{g}{57.3}\cos\gamma_t \\ M'_\theta & M'_V & M'_q & M'_\alpha \\ Z_\theta & Z_V - \frac{57.3 g \cos\gamma_t}{V_t^2} & 1 + Z_q & Z_\alpha + \frac{g}{V_t}\sin\gamma_t \end{bmatrix} \begin{bmatrix} \Delta\theta \\ \Delta V \\ q \\ \Delta\alpha \end{bmatrix} + \begin{bmatrix} 0 & 0 \\ X_{\delta_e} & X_0 \\ M'_{\delta_e} & M'_0 \\ Z_{\delta_e} & Z_0 \end{bmatrix} \begin{bmatrix} \Delta\delta_e \\ 1 \end{bmatrix}$$

Measurement System:

$$\Delta\theta_m = \Delta\theta + \theta_b \quad \text{(deg)}$$

$$\Delta V_m = \Delta V + V_b \quad \text{(ft/sec)}$$

$$q_m = q + q_b \quad \text{(deg/sec)}$$

$$\Delta\alpha_m = \alpha - \frac{23.1}{V_t}\cos\alpha_t\, q + \alpha_b \quad \text{(deg)}$$

$$\Delta a_{z_m} = \frac{V_t}{57.3}\left(\dot{\alpha} - Z_\theta \Delta\theta - q\right) + a_{z_b} \quad \text{(ft/sec}^2\text{)}$$

$$\dot{q}_{1m} = \dot{q} + \dot{q}_{1_b} \quad \text{(deg/sec}^2\text{)}$$

$$\Delta a_{x_m} = \dot{V} - X_\theta \Delta\theta + a_{x_b} \quad \text{(ft/sec}^2\text{)}$$

$$\dot{q}_{2m} = \dot{q} + \dot{q}_{2_b} \quad \text{(deg/sec}^2\text{)}$$

Definitions:

$$X_\theta \equiv -\frac{g}{57.3}\cos\gamma_t$$

$$Z_0 = -\frac{g}{V_t}\sin\gamma_t \approx 0$$

$$Z_V \approx -\frac{57.3}{V_t^2}\, g \cos\gamma_t$$

TABLE 2

SUMMARY OF FLIGHT DATA

	Record Number	V_{trim} (fps)	α_{trim} (deg)	δ_e - Input Type	Record Length (seconds)
Low Speed M = .212 Sea Level	2*	266.5	5.8	Oscillatory type sine wave - short period only	12.
	5	255.7	5.2	Oscillatory type - short period only	11.
	6	251.6	5.9	Pulse	61.
High Speed M = .63 10,000 ft.	10	683.7	.3	Pulse-short period only	12.
	12	669.9	.2	Pulse	84.
	13	680.8	.1	Double doublet type - short period only	13.
	18	682.8	-.7	Double pulse type - short period only	10.
	19	690.0	-.8	Persistent pulse type	26.

* Pilot indicated moderate turbulence present

TABLE 3

INITIAL PARAMETER ESTIMATES

Para.	Low Speed V_t =236	V_t =266.5	V_t =253.5	High Speed V_t =679
*X_θ	-.56147	-.56147	-.56147	-.56147
X_V	-.046	-.0519	-.049	-.016
X_α	-.1615	-.205	-.1723	-1.2
*M'_θ	0.	0.	0.	0.
M'_V	.0347	.031	.032	.113
M'_q	-1.95	-2.20	-2.09	-4.96
M'_α	-4.59	-5.85	-5.30	-18.6
M'_{δ_e}	-9.63	-12.28	-11.11	-51.8
*Z_θ	0.	0.	0.	0.
*Z_V	-.0331	-.026	-.0287	-.004
Z_q	0.	0.	0.	0.
Z_α	-.974	-1.242	-1.124	-2.46
Z_{δ_e}	-.102	-.13	-.118	-.18

* Parameters assumed known sufficiently accurate to fix

TABLE 4

MEASUREMENT NOISE STATISTICS FROM

SAMPLE VARIANCE COMPUTATION

Standard Deviations (σ)

σ_θ	= .05 deg
σ_V	= 1.4 fps
σ_q	= .1 deg/sec
σ_α	= .16 deg
σ_{a_z}	= 3.46 ft/sec^2
$\sigma_{\dot{q}}$	= 2.3 deg/sec^2
σ_{a_x}	= .8 ft/sec^2
σ_{q_2}	= 6.2 deg/sec^2

TABLE 5

IDENTIFICATION RESULTS - RECORD No. 2 ($Q = 0$)

Para.	Initial Estimates	2-1 (a_x)	2-2 (R-Int)	2-3 (R-Adj)	2-4 (R-Adj)	2-5 ($\hat{R}$)	$2\sigma_f$ (2-5)
X_V	-.052	.05	-.134	.094	-.074	-.104	.044
X_α	-.205	-.386	-.102	-.121	-.185	-.168	.22
X_{δ_e}	0.	.325	fix	fix	fix	fix	
M'_θ	0.	fix	fix	fix	fix	fix	
M'_V	.031	fix	fix	fix	fix	fix	
M'_q	-2.20	-2.08	-2.05	-2.16	-1.81	-2.03	.104
M'_α	-5.85	-4.53	-4.64	-4.38	-5.23	-4.67	.108
M'_{δ_e}	-12.28	-10.58	-10.58	-10.56	-9.75	-10.05	.3
Z_V	-.026	fix	fix	fix	fix	fix	
Z_α	-1.242	-1.108	-1.126	-1.01	-1.19	-1.04	.046
Z_{δ_e}	-.13	-.44	-.36	-.33	-.137	-.223	.7
σ_θ		.05	.05	.1	.1	.2	
σ_V		1.4	1.4	1.4	1.4	1.7	
σ_q		.1	.1	.2	.2	.5	Measurement Noise
σ_α		.16	.16	.16	.5	.4	
σ_{a_z}		3.5	3.5	4.5	3.0	4.8	
$\sigma_{\dot{q}}$		4.6	2.3	3.0	3.0	3.7	
σ_{a_x}		.8	NA	NA	NA	NA	

Notes: 1. Fixed $X_\theta = -.561$, $Z_\theta = X_q = Z_q = 0$ for all runs

2. X_o , M'_o , Z_o , q_b , a_{z_b}, $\dot{q}_b$, a_{x_b} also identified

Fix - fixed at initial estimate

TABLE 6

IDENTIFICATION RESULTS - RECORD No. 5 ($Q = 0$)

Para.	Initial Estimates	5-1 (a_x)	5-2 (R - Int)	5-3 (R-Adj)	5-4 (R-Adj)	5-5 ($\hat{R}$)	$2\sigma_f$ (5-5)
X_v	-.049	-.11	fix	fix	fix	fix	
X_α	-.172	-.25	-.093	-.051	-.096	.014	.152
X_{δ_e}	0.	.14	fix	fix	fix	fix	
M'_θ	0.	fix	fix	fix	fix	fix	
M'_v	.032	fix	fix	fix	fix	fix	
M'_q	-2.09	-1.98	-2.01	-2.21	-1.72	-2.34	.124
M'_α	-5.3	-5.25	-5.29	-4.84	-5.91	-4.86	.096
M'_{δ_e}	-11.11	-10.16	-10.27	-10.51	-9.43	-10.77	.342
Z_v	-.0287	fix	fix	fix	fix	fix	
Z_α	-1.124	-1.19	-1.18	-1.07	-1.25	-.998	.040
Z_{δ_e}	-.118	-.246	-.199	-.323	.002	-.235	.056
σ_θ		.05	.05	.1	.1	.25	
σ_v		1.4	1.4	1.4	1.4	1.8	
σ_q		.1	.1	.2	.2	.68	
σ_α		.16	.16	.16	.5	.3	
σ_{a_z}		3.5	3.5	4.5	3.0	3.5	
$\sigma_{\dot{q}}$		4.6	2.3	3.0	3.0	4.2	
σ_{a_x}		.8	NA	NA	NA	NA	

Measurement Noise

Notes: 1. Fixed $X_\theta = -.561$, $Z_\theta = X_q = Z_q = 0$ for all runs

2. X_0 , M'_0 , Z_0 , q_b , a_{z_b}, $\dot{q}_b$, a_{x_b} also identified

Fix - fixed at initial estimate

TABLE 7

IDENTIFICATION RESULTS - RECORD No. 6 ($Q = 0$)

Para.	Initial Estimates	6-1 (5 sec)	6-2 (5 sec)	6-3 (δ_e - mod) (14 sec)	6-4 (δ_e - mod) (14 sec, $\hat{R}$)	$2\sigma_f$ (6-4)	6-5 (δ_e - mod) (28 sec)	
X_v	-.049	fix	fix	-.041	-.037	.0028	-.023	
X_α	-.172	-.242	-.213	-.211	-.181	.08	(6-3)	
X_{δ_e}	0.	fix	fix	fix	fix		fix	
M'_θ	0.	fix	fix	fix	fix		fix	
M'_v	.032	fix	fix	fix	fix		-.014	
M'_q	-2.09	-2.08	-2.2	-1.97	-1.99	.074	(6-3)	
M'_α	-5.3	-4.57	-4.36	-4.88	-4.74	.056	(6-3)	
M'_{δ_e}	-11.11	-9.32	-9.9	-9.87	-9.76	.22	(6-3)	
Z_v	-.0291	fix	fix	fix	fix		fix	
Z_α	-1.124	-1.02	-.994	-1.097	-1.04	.028	(6-3)	
Z_{δ_e}	-.118	-.12	-.32	-.346	-.309	.06	(6-3)	
σ_θ		.05	.1	.05	.08		.05	Measurement Noise
σ_v		1.4	1.4	1.4	1.7		1.4	
σ_q		.1	.2	.1	.28		.1	
σ_α		.16	.16	.16	.19		.16	
σ_{a_z}		3.5	4.5	3.5	4.		3.5	
$\sigma_{\dot{q}}$		2.3	3.0	3.0	4.1		3.	
σ_{a_x}		NA	NA	NA	NA		NA	

Notes: 1. Fixed $X_\theta = -.561$, $Z_\theta = X_q = Z_q = 0$ for all runs

2. X_θ, M'_θ, Z_o, q_b, a_{z_b}, $\dot{q}_b$, a_{x_b} also identified

Fix - fixed at initial estimate unless otherwise indicated

TABLE 8

IDENTIFICATION RESULTS - RECORD NO. 5

($Q \neq 0$ and δ_e UNFILTERED)

Para.	*Initial Estimates	5,6 $(Q, \hat{R})$	$2\sigma_f$ (5,6)	
M'_q	-2.09	-2.02	.154	
M'_α	-5.3	-4.41	.104	
M'_{δ_e}	-11.11	-9.35	.444	
Z_α	-1.124	-.98	.026	
Z_{δ_e}	-.118	-.43	.04	
σ_θ		.08		Measurement Noise
σ_v		1.9		
σ_q		.32		
σ_α		.2		
σ_{a_y}		4.1		
σ_{δ_e}		.14		Process Noise

*Parameters not shown held fixed (Refer to Tables 3 and 6.)

TABLE 9

IDENTIFICATION RESULTS (HIGH SPEED)

RECORDS 13, 18, and 19

Para.	*Initial Estimates	13-1 (Q, R)	$2\sigma_f$ 13-1	18-1 $(Q, \hat{R})$	$2\sigma_f$ 18-1	19-1 $(Q=0)$	$2\sigma_f$ 19-1
X_α	-1.2	fix		fix		-.652	.27
M'_q	-4.96	-4.03	.76	-1.41	.46	-3.12	.22
M'_α	-18.6	-18.59	1.36	-31.6	1.2	-31.3	.67
M'_{δ_e}	-51.8	-20.12	2.0	-16.94	1.74	-29.05	.88
Z_α	-2.46	-2.93	.11	-2.85	.14	-3.10	.07
Z_{δ_e}	-.18	.21	.06	.09	.08	fix	
σ_θ		.12		.19		.2	
σ_v		1.6		1.9		1.9	
σ_q		.91		1.49		.6	
σ_α		.09		.32		.4	
σ_{a_z}		3.8		7.2		5.	
σ_{δ_e}		.14		.14		0.	

* Parameters not shown held fixed (Refer to Table 3.)

Appendix A

IDENTIFICATION ALGORITHM

This appendix summarizes the iterated Kalman filter/fixed-point Smoother Identification Algorithm.

Problem Statement

Consider the general mathematical model representing the equations of motion of the aircraft (or other dynamics of importance)

$$\dot{x} = f(x, p, u) + g(x, p)\, w(t), \qquad x(t_0) = x_0$$
$$\dot{p} = 0 \tag{A-1}$$

and the measurement system model by

$$y_i = h(x_i, p, u_i) + v_i, \qquad i = 0, 1, \cdots, N \tag{A-2}$$

where

- x - state vector for the aircraft (v , q , α , etc.)
- p - unknown parameter vector (M_q , M_α, etc.)
- u - control input (δ_H or x_p , etc.)
- y_i - measurement vector of sensor outputs at discrete points in time
- $f(\,), h(\,), g(\,)$ - functional form of aircraft and measurement system
- x_0 - initial condition

and $w(t)$ and v_i are independent random noise vectors, which are appropriately called process and measurement noise, respectively, and are chosen as white, Gaussian and zero mean for analytical simplicity with the following covariance matrices:

$$E\left\{ w(t)\, w^T(t+\tau) \right\} = Q\delta(\tau)$$

$$E\left\{ v_i\, v_i^T \right\} = R\delta_{ij}$$

Also, the aircraft initial condition, x_0 , and initial estimate of the parameter vector, p_0 , are assumed Gaussian random variables with covariance matrix, P_0 ; which is a measure of the accuracy of the "a priori" estimates of x_0 and p_0 . Note that P_0 is the covariance matrix of the augmented state vector, $(x_0^T : p_0^T)^T$.

The problem can now be stated formally: given the measurement data, y_i , and the control input, u_i , for $i = 0, 1, \ldots, N$, obtain the best estimate of x_0 and p , for the mathematical model chosen. The mathematical model as used here implies both the structural forms for $f(\ )$, $g(\ )$, and, $h(\ )$ and also the selected values for the Q and R covariance matrices. The best estimate will, in general, depend upon the criteria used to determine the best estimate. Bayesian estimation philosophy is used here and the best estimate denotes that estimate which minimizes the mean square error criterion (i.e., the unbiased and minimum variance estimate).

The solution to the problem as stated above is that of obtaining the fixed-point smoothed estimate of the initial augmented state, $x_{a_0} \triangleq (x_0^T : P_0^T)^T$ which is the conditional expectation, $E\{x_{a_0} / Y(N)\}$, where $Y(N) \triangleq [y_1^T, y_2^T \cdots y_N^T]^T$. With appropriate Gaussianity assumptions, this problem is solved by using an iterated Kalman filter/fixed-point smoother technique.

Iterated Kalman Filter Algorithm

With reference to Equations (A-1) and (A-2), the iterated Kalman filter algorithm is summarized below between the arbitrary data points at the time t_{i-1} and t_i . Also note that x is interpreted as the augmented state vector, i.e., $x \triangleq (x^T p^T)^T$.

$$\hat{x}_{i/i}^{(j+1)} = \hat{x}_{i/i-1}^{(j)} + \psi_i^{(j)} \cdot \tilde{z}_i^{(j)} \qquad \text{(augmented state estimates)}$$

$$\hat{x}_{i/i-1}^{(j)} = \int_{t_{i-1}}^{t_i} f(x,u)\,dt + \Phi_{i,i-1}^{(j)} \left[\hat{x}_{i-1/i-1} - \hat{x}_{i-1/i}^{(j)} \right] \qquad \text{(predicted state estimate)}$$

$$P^{(j)}_{i/i-1} = \Phi^{(j)}_{i,i-1} P_{i-1} \Phi^{(j)T}_{i,i-1} + \bar{Q}$$ (predicted error covariance matrix)

$$\psi^{(j)}_i = P^{(j)}_{i/i-1} H^{(j)T}_i \left[H^{(j)}_i P^{(j)}_{i/i-1} H^{(j)T}_i + R \right]^{-1}$$ (Kalman gain matrix)

$$\hat{x}^{(j+1)}_{i-1/i} = \hat{x}_{i-1/i-1} + P_{i-1} \Phi^{(j)T}_{i,i-1} H^{(j)T}_i \left[H^{(j)}_i P^{(j)}_{i/i-1} H^{(j)T}_i + R \right]^{-1} \cdot \tilde{z}^{(j)}_i$$

(one-state smoothed estimate)

$$P^{(j)}_i = \left[I - \psi^{(j)}_i H^{(j)}_i \right] P^{(j)}_{i/i-1}$$ (covariance matrix of state estimation errors)

where

$$\Phi^{(j)}_{i,i-1} \triangleq I + \left. \frac{\partial f}{\partial x} \right|_{\hat{x}^{(j)}_{i-1/i}} \cdot \Delta t + \frac{1}{2} \left(\frac{\partial f}{\partial x} \right)^2 \Delta t^2 + \cdots$$ (transition matrix)

$$\bar{Q} \triangleq \Gamma Q \Gamma^T \Delta T$$

$$\Gamma \triangleq \begin{bmatrix} \frac{g}{0} \end{bmatrix}$$

$$H^{(j)}_i \triangleq \left. \frac{\partial h}{\partial x} \right|_{\hat{x}^{(j)}_{i/i}}$$ (linearized output matrix)

$$\tilde{z}^{(j)}_i \triangleq y_i - h_i \left(\hat{x}^{(j)}_{i/i} \right) - H^{(j)}_i \left\{ \hat{x}^{(j)}_{i/i-1} - \hat{x}^{(j)}_{i/i} \right\}$$ (predicted residuals)

Δt = sample time = $t_i - t_{i-1}$

and at the initial or starting conditions

$$\hat{x}^{(1)}_{i-1/i} = \hat{x}_{i-1/i-1} \cdot \hat{x}^{(1)}_{i/i} = \hat{x}^{(1)}_{i/i-1}$$

The iteration scheme starts with $j = 1$ and terminates when $x_{i/i}^{(j)} \approx x_{i/i}^{(j-1)}$ or after a prespecified number of iterations, usually one in practice. The converged values of $\hat{x}_{i/i}^{(j)}$, $\hat{x}_{i-1/i}^{(j-1)}$ and $P_i^{(j-1)}$ are taken as the estimates $\hat{x}_{i/i}$, $\hat{x}_{i-1/i}$ and the covariance P_i, respectively, for the next data point.

Although not directly a part of the algorithm, the covariance of the predicted residuals is given by:

$$cov\left(\tilde{z}_i^{(j)}\right) = R + H_i^{(j)} P_{i/i-1}^{(j)} H_i^{(j)T}$$

This is the theoretically calculated covariance of the residual sequence and it can be used to detect modelling deficiencies by checking to see if the actual statistics of the residuals are consistent with this calculation.

Fixed-Point Smoother Algorithm

$$\hat{x}_{o/i} = \hat{x}_{o/i-1} + B_i H_i^{(f)T} R^{-1} \tilde{z}_i^{(f)} \qquad \text{(fixed-point smoother estimate)}$$

$$P_{o/i} = P_{o/i-1} - B_i H_i^{(f)T} R^{-1} H_i^{(f)} \Phi_{i,i-1}^{(f)} B_{i-1}^T \qquad \text{(covariance of fixed-point smoothed estimation error)}$$

where

$$B_i = B_{i-1} \Phi_{i,i-1}^{(f)T} \left[I - \psi_i^{(f)} H_i^{(f)}\right]^T, \qquad B_0 = P_0$$

Note that $P_{o/i}$ is not needed to compute $\hat{x}_{o/i}$ and that the superscript (f) denotes the last value of the particular matrix from the iterated Kalman filter algorithm.

Suboptimal Q and R Estimators

The recursive form of the Q and R estimators, which are developed using covariance matching techniques, are given in the following:

$$\hat{R}_{i/i} = \frac{1}{i}\left[(i-1)\,\hat{R}_{i-1/i-1} + \tilde{z}_i \tilde{z}_i^T - H_i P_{i/i-1} H_i^T\right]$$

$$\hat{\bar{Q}}_{i/i} = \frac{1}{i}\left[(i-1)\,\hat{\bar{Q}}_{i-1/i-1} + \psi_i \tilde{z}_i \tilde{z}_i^T \psi_i^T + P_i - \Phi_{i,i-1} P_{i-1} \Phi_{i,i-1}^T\right]$$

for $i = 1, \ldots, N$